Clim. Past, 21, 1–19, 2025 https://doi.org/10.5194/cp-21-1-2025 © Author(s) 2025. This work is distributed under the Creative Commons Attribution 4.0 License.





# East Greenland Ice Sheet retreat history from Scoresby Sund and Storstrømmen Glacier during the last deglaciation

Jacob T. H. Anderson<sup>1</sup>, Nicolás E. Young<sup>1</sup>, Allie Balter-Kennedy<sup>1</sup>, Karlee K. Prince<sup>2</sup>, Caleb K. Walcott-George<sup>2,3</sup>, Brandon L. Graham<sup>4</sup>, Joanna Charton<sup>1</sup>, Jason P. Briner<sup>2</sup>, and Joerg M. Schaefer<sup>1</sup>

**Correspondence:** Jacob T. H. Anderson (janderson@ldeo.columbia.edu)

Received: 11 June 2025 – Discussion started: 30 June 2025

Revised: 18 September 2025 – Accepted: 22 September 2025 – Published:

**Abstract.** The lack of geological constraints on past icesheet change in marine-based sectors of the Greenland Ice Sheet (GrIS) following the Last Glacial Maximum limits our ability to assess (1) the drivers of ice-sheet change, and (2) the performance of ice-sheet models that are benchmarked against the paleo-record of GrIS change. Here, we provide new in situ <sup>10</sup>Be surface exposure chronologies of ice-sheet margin retreat from the outer Scoresby Sund and Storstrømmen Glacier regions in eastern and northeastern Greenland, respectively. Ice retreated from Rathbone Island. east of Scoresby Sund, by  $\sim 14.1$  ka, recording some of the earliest documentations of terrestrial deglaciation in Greenland. The mouth of Scoresby Sund deglaciated by  $\sim 13.2$  ka, and retreated at an average rate of  $\sim 43 \,\mathrm{m\,yr^{-1}}$  between 13.2 and 9.7 ka. Storstrømmen Glacier retreated from the outer coast to within  $\sim 3 \, \text{km}$  of the modern ice margin between  $\sim$  12.7 and 8.6 ka at an average rate of  $\sim$  28 m yr<sup>-1</sup>. Retreat then slowed or reached a stillstand as ice retreated  $\sim$  3 km between  $\sim 8.6$  ka to the modern ice margin at  $\sim 8.0$  ka. These retreat rates are consistent with late glacial and Holocene estimates for marine-terminating outlet glaciers across East Greenland, and comparable to modern retreat rates observed at the largest ice streams in northeastern, and northwestern Greenland.

#### 1 Introduction

The rate of Greenland Ice Sheet (GrIS) mass loss and contribution to sea-level rise has increased over recent decades (Khan et al., 2022; The IMBIE Team, 2020). Projections under varying warming scenarios suggest that GrIS contributions to global mean sea level by 2100 range from -0.02 to 0.15 m to 0.05-0.23 m under SSP1-2.6 and SSP5-8.5 scenarios, respectively (IPCC, 2021). To place these contemporary short-term ice sheet dynamics in context, we examine retreat patterns of the GrIS since the Last Glacial Maximum (LGM; 26.5-19 ka; Clark et al., 2009).

Previous research has provided robust constraints on the timing and pattern of deglaciation in southwestern Greenland (e.g., Briner et al., 2020; Larsen et al., 2014; Lesnek et al., 2020; Levy et al., 2012; Young et al., 2011, 2020, 2021). Relying partly on these detailed constraints, Briner et al. (2020) suggested rates of southwestern GrIS mass loss, and perhaps the entire GrIS, over the twenty-first century are predicted to exceed rates experienced anytime in the last 12,000 years. Comparable geologic records from eastern (e.g., Larsen et al., 2020; 2022; Levy et al., 2016; Roberts et al., 2024) and fewer studies from northern (e.g. Kelly and Bennike, 1992; O'Regan et al., 2021) sectors of Greenland, have been used to constrain the timing and rates of ice sheet margin retreat during the last deglaciation. In some regions across East and North Greenland, however, data gaps hinder our ability to reconstruct the pattern and timing of GrIS retreat, and assess the accuracy of ice sheet models. This

<sup>&</sup>lt;sup>1</sup>Lamont-Doherty Earth Observatory, Columbia University, Palisades, NY, USA

<sup>&</sup>lt;sup>2</sup>Department of Earth Sciences, University at Buffalo, Buffalo, NY, USA

<sup>&</sup>lt;sup>3</sup>University of Kentucky, Department of Earth and Environmental Sciences, Lexington, KY, USA

<sup>&</sup>lt;sup>4</sup>United States Geological Survey, Florence Bascom Geoscience Center, Reston, VA, USA

is particularly important in northeast Greenland, where major marine-terminating ice streams drain large portions of the GrIS. For example, the Northeast Greenland Ice Stream (NEGIS) is one of the largest drainage systems in Greenland, accounting for  $\sim\!16\,\%$  of the total GrIS discharge through three major marine-terminating outlet glaciers: Nioghalvfjerdsfjord Glacier (79° N Glacier), Zachariae Isstrøm, and Storstrømmen Glacier (Hvidberg et al., 2020). Collectively, these glaciers contain 1.4 m of sea level equivalent (An et al., 2021; Rignot et al., 2022).

During the LGM, the East GrIS extended onto the continental shelf edge, with significant contributions of ice from expanded marine terminating ice streams such as NEGIS and in the Scoresby Sund region (Fig. 1). Marine geological data and geophysical surveys identifying glacial lineations and recessional moraines have been used to reconstruct patterns of ice sheet retreat along the continental shelf during the last deglaciation (Arndt et al., 2015, 2017; Evans et al., 2009; López-Quirós et al., 2024; Ó Cofaigh et al., 2004, 2025; Stein et al., 1996). On the northeast Greenland shelf, radiocarbon dates from marine sediments show that ice sheet retreat was underway on the shelf edge by 21.6 cal ka BP at Norske Trough, and by 19 cal ka BP at Westwind Trough (Ó Cofaigh et al., 2025). Ice retreated to the mid-shelf before 18.6 cal ka BP (O Cofaigh et al., 2025), and that ice retreated from the inner continental shelf east of NEGIS between 13.4–12.5 cal ka BP, which was primarily driven by an influx of relatively warm Atlantic water (Davies et al., 2022; Hansen et al., 2022). The NEGIS retreated from the outer coast to the present ice margin between 11.7 and  $\sim$  9.0 ka (Larsen et al., 2018; Roberts et al., 2024).

Despite recent advances understanding the retreat history from the outer coastline to the modern ice margin of marineterminating glaciers along eastern Greenland (e.g., Håkansson et al., 2007a; Larsen et al., 2020, 2022; Levy et al., 2016), there are still major gaps in some regions (i.e., a lack of consistent ages or an absence of dated material). To record ice margin change, glacial landforms (such as erratic boulders and glacially polished bedrock) can be dated via in situ cosmogenic nuclides produced in rock surfaces (e.g. Ivy-Ochs and Briner, 2014; Lal, 1991; Nishiizumi et al., 1989). Here, we build on previous work studying the retreat history of marine-terminating glaciers in East Greenland, and present in situ cosmogenic <sup>10</sup>Be exposure ages from (i) the outer coast of Scoresby Sund, which improve age constraints at the mouth of the largest fjord system in Greenland, and (ii) near the modern ice margin of Storstrømmen Glacier, where few existing ages constrain East GrIS retreat. We integrate these data to calculate rates of ice margin retreat, and reconstruct a detailed East GrIS retreat pattern that we connect to potential mechanisms driving these GrIS changes.

## 2 Study sites and geological setting

The eastern margin of Greenland, from 79° N Glacier in the north, to Scoresby Sund in the south, comprises an extensive system of marine-terminating outlet glaciers, ice-free valleys, and fjords at lower elevations that transect blockfieldcovered plateaus at higher elevations (Skov et al., 2020). Retreat of the ice margin along East Greenland has been constrained by marine and terrestrial radiocarbon ages (Table 1) and surface exposure ages (Fig. 1). Along the eastern margin of Greenland, the ice-free landscapes comprise moraines, erratic boulders and polished bedrock surfaces that can be directly dated via cosmogenic nuclide exposure dating (e.g., Larsen et al., 2022; Levy et al., 2016; Skov et al., 2020). Grounded ice between Peary Land, 79° N Glacier, and Zachariae Isstrøm retreated westward out of the Greenland Sea and reached the present-day outer coastline by  $\sim 11.4 \,\mathrm{ka}$ (Larsen et al., 2020). Between Storstrømmen Glacier and Kong Oscar Fjord, the GrIS receded to the outer coast between  $\sim$  12.8 and 11.5 ka (Håkansson et al., 2007b; Larsen et al., 2022; Skov et al., 2020). The ice sheet subsequently retreated from the outer coast toward intermediate sites on the northeastern margin between  $\sim 11-9$  ka (Larsen et al., 2018, 2022; Skov et al., 2020). The 79° N Glacier experienced slow early Holocene ice margin retreat from the outer coast to the present ice margin (Larsen et al., 2018; Bennike and Weidick, 2001). However, retreat rates from the inner fjord suggest rapid deglaciation between 10 and 8.5 ka (Roberts et al., 2024). Ice reached close to the modern ice margin by ~9 ka at Lambert Land and had retreated to Borgfjorden by  $\sim 8.9 \, \text{ka}$  in the Dove Bugt region, and Vandrepasset by  $\sim$  8.6 ka in Bessel Fjord (Larsen et al., 2018, 2022).

A combination of raised marine beaches and terrestrial geological evidence has provided retreat chronologies of the East GrIS from the outer coast to the present-day ice margin (Fig. 1, Leger et al., 2024). Geomorphological mapping and dating glacial landforms and deposits using terrestrial cosmogenic nuclides (TCN; in situ <sup>10</sup>Be) and radiocarbon ages have provided direct constraints of ice margin retreat (e.g. Håkansson et al., 2007a; Larsen et al., 2022; Levy et al., 2016). Our study sites focus on the glacial geology of two marine embayments: Scoresby Sund and Dove Bugt (Figs. 1, 2).

## 2.1 Scoresby Sund

Scoresby Sund (Kangertittivaq) is a large (13 700 km²) fjord system situated between Jameson Land and Liverpool Land in the north, King Christian IX Land in the south, and Milne Land, and the Renland Peninsula in the west (Fig. 3). The fjord system extends  $\sim 350 \, \mathrm{km}$  inland from the outer coast (Dowdeswell et al., 1994), with the outer fjord being  $\sim 120 \, \mathrm{km}$  long, up to 50 km wide, and up to 650 m deep. Scoresby Sund is deepest in the south and gently rises to the north towards Jameson Land (Håkansson et al., 2007a). At

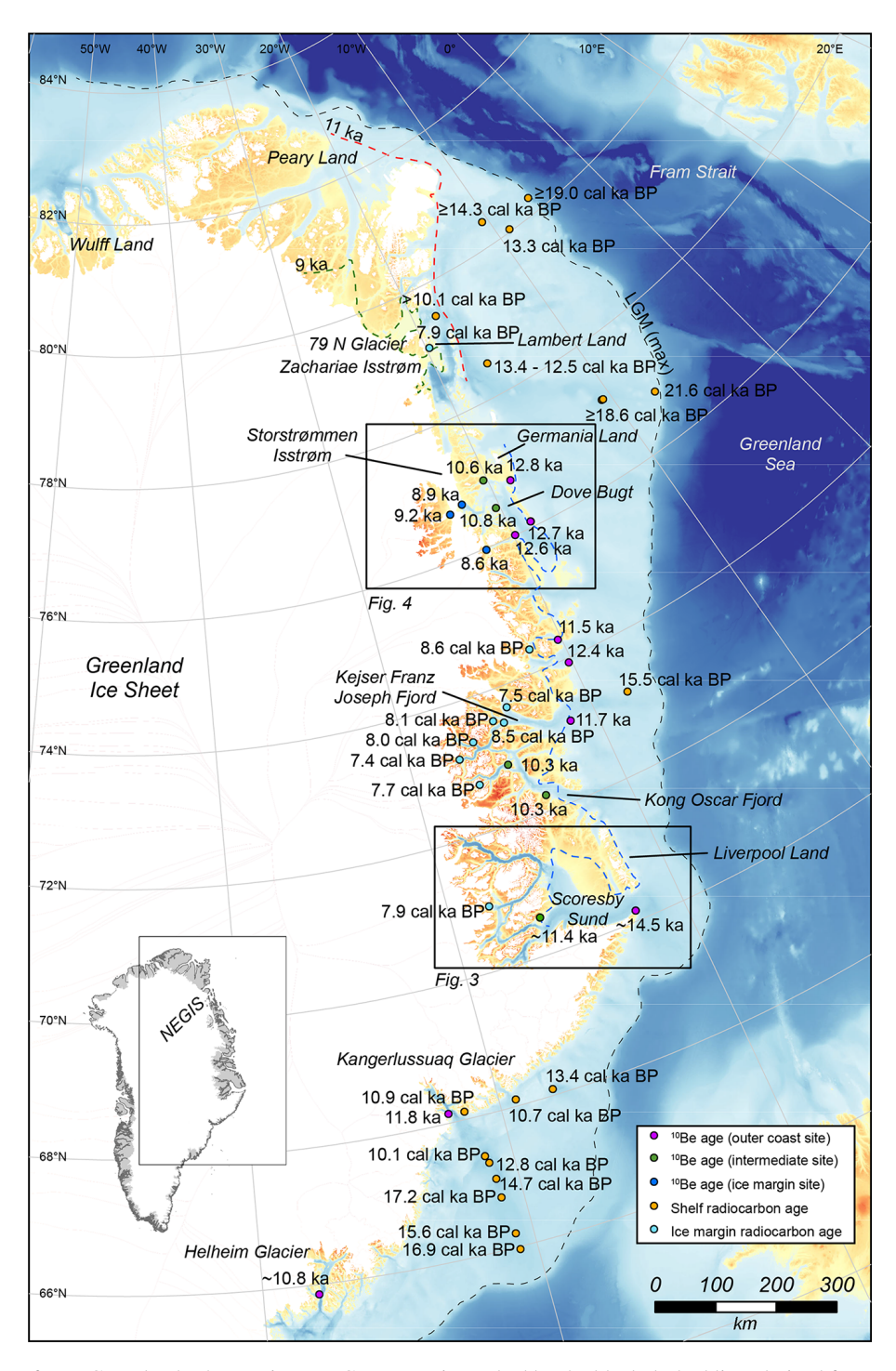


Figure 1. Study area of East Greenland. The maximum LGM extent is marked by the black dashed line, derived from Leger et al. (2024 and references therein). The Milne Land stade moraines are marked by the blue line (Funder et al., 2011; Larsen et al., 2022). The ice margin at  $\sim$  11 and 9 ka is marked by the red and green dashed lines, derived from Larsen et al. (2020). Previously reported <sup>10</sup>Be ages from outer coast, intermediate and ice margin sites (Dyke et al., 2014; Håkansson et al., 2007a; Hughes et al., 2012; Larsen et al., 2022; Levy et al., 2016). Radiocarbon ages are listed in Table 1. The black rectangles show the locations of Scoresby Sund (Fig. 3) and Dove Bugt region (Fig. 4). Basemap derived from IBCAO bathymetry (Jakobsson et al., 2024).

**Table 1.** Radiocarbon ages from eastern Greenland.

Sample number	Latitude	Longitude	e Location	Material dated	Radiocarbon age ( <sup>14</sup> C yr BP)	Radiocarbon age uncertainty $(1\sigma)$	Calibrated age (cal yr BP, median)	Calibrated age range (cal yr BP, 2σ)	Reference
Northeast Greenl	and shelf					(10)	iliculaii)	(car yr B1, 20)	
		9 022	DA17 NC	Mixed	12.070	60	12 201*	13 202-	Uoncon at
ETH-106030	80.037	-8.923	DA17-NG- ST03-039G	planktonic foraminifera	12 070	60	13 291*	13 584*	Hansen et al. (2022)
ETH-113888	78.501	-16.28	DA17-NG- ST08-092G	Mixed benthic foraminifera	10 200	190	12 473*	11 268– 12 595*	Davies et al. (2022)
AWI 2795.1.1	77.497	-18.14	PS100/270	Mixed benthic foraminifera	9437	104	10 138	9670–10 568	Syring et al. (2020)
121 063.1.1	77.127	-10.68	DA17-NG- ST12–135G	Mixed benthic foraminifera	14 450	220	16 684	16 080–17 285	López-Quirós et al. (2024)
Lambert Land									
442 909	79.107	-19.75	Zachariae Isstrom	Marine bivalve	7595	55	7905	7624–8184	Bennike and Weidick (2001
Clavering Ø									
I-9659	74.350	-21.87	Clavering Ø	Marine bivalve	8195	125	8148	7050–9396	Weidick (1978
Kejser Franz Jose	ph Fjord						·	·	·
MM/G3	73.550	-25.12	Kejser Franz Joseph Fjord	Marine bivalve	8020	100	8078	7179–9086	Wagner and Melles (2002)
60 282.1.1	73.675167	-24.18	HH13-012	Mixed benthic foram	7470	130	7471	6518–8376	Olsen et al. (2022)
4491.1.1	73.474667	-24.61	PS2633	Foraminifera	8376	84	8452	7550–9447	Olsen et al. (2022)
PS2630	73.158	-18.07	PS2630	Foraminifera	13 560	130	15 544	15 113–15 989	Evans et al. (2002)
Kong Oscar Fjord	i								
I-9104	73.350	-26.47	Kong Oscar Fjord	Marine bivalve	7760	115	7985	7654–8329	Weidick (1977
I-9658	73.167	-27.42	Kong Oscar Fjord	Marine bivalve	7160	125	7428	7067–7779	Weidick (1978
Lu-1070	72.717	-26.83	Kong Oscar Fjord	Marine bivalve	7530	75	7698	7150–8297	Håkansson (1976)
Scoresby Sund									
UtC-7428	70.595	-21.54	Scoresby Sund	Plant macrofossil	8900	50	10 026	9887–10 197	Cremer et al. (2001)
AAR-199	70.338	-23.71	PS1715-1	Foraminifera	10 340	150	11 250	10 674–11 819	Marienfeld (1991)
AAR-200	70.483	-24.67	PS1719-1	Foraminifera	10 480	190	11 645	11 058-12 392	Marienfeld (1991)
AAR-202	70.708	-25.00	PS1728-1	Foraminifera	10 760	120	12 023	11 503–12 486	Marienfeld (1991)
AAR-201	70.928	-24.98	PS1727-1	Foraminifera	9080	650	9589	7952–11272	Marienfeld (1991), Dowdeswell e al. (1994)
K-1461	71.167	-25.33	Scoresby Sund	Marine bivalve	9040	140	9650	9275-10 108	Funder (1990)
K-3109	70.500	-23.45	Scoresby Sund	Marine bivalve	10560	145	11 726	11 199–12 318	Funder (1990)
AAR-636	70.533	-23.63	Scoresby Sund	Marine bivalve	9170	140	9764	9398–10183	Gulliksen et al. (1991)
I-9492	70.500	-26.18	Scoresby Sund	Marine bivalve	9925	140	10 882	10 395-11 310	Funder (1978)
AAR-3368	70.387	-23.87	Scoresby Sund	Plant macrofossils	9780	160	11 186	10 695–11 743	Hansen (2001)

 Table 1. Continued.

Sample number	Latitude	Longitude	e Location	Material dated	Radiocarbon age ( <sup>14</sup> C yr BP)	Radiocarbon age uncertainty $(1\sigma)$	Calibrated age (cal yr BP, median)	Calibrated age range (cal yr BP, 2σ)	Reference
100 380, 100 381	70.843	-24.01	Scoresby Sund	Plant macrofossils	9665	55	11 058	10 780–11 207	Bennike et al. (1999)
AAR-2540	70.850	-24.02	Scoresby Sund	Plant macrofossils	10 130	130	11 729	11 257–12 177	Bennike et al. (1999)
AAR-3369	70.850	-24.07	Scoresby Sund	Plant macrofossils	9440	65	10 681	10 501–11 069	Hansen (2001
AAR-3802	70.850	-24.15	Scoresby Sund	Marine bivalve	9985	60	10915	10 581-11 203	Hansen (2001
AAR-2571	70.985	-24.00	Scoresby Sund	Plant macrofossils	7900	100	8751	8464–9006	Böcher and Bennike (1996
AAR-1829	70.95944	4 –24.1136	1Scoresby Sund	Marine bivalve	10 140	100	11 126	10 696–11 557	Funder and Hansen (1996
AAR-2541	70.950	-24.12	Scoresby Sund	Plant macrofossils	9910	130	11 411	10 885-11 873	Hansen (2001
AAR-644	70.914	-24.21	Scoresby Sund	Marine bivalve	9670	180	10 486	9930–11 085	Ingolfsson et al. (1994)
87516	71.567	-23.97	Scoresby Sund	Plant macrofossils	7000	390	7848	7003–8601	Böcher and Bennike (1996), Bennike et al. (1999)
K-1915	71.350	-24.83	Scoresby Sund	Marine bivalve	10300	120	11 423	11 018-11 902	Funder (1978)
I-5421	70.950	-28.15	Scoresby Sund	Marine bivalve	7540	130	7863	7560-8182	Funder (1978)
Kangerlussuaq Ti	rough								
AA-4026	66.203	-30.66	10A	Foraminifera	13585	110	15 628	15 259–15 995	Williams (1993)
AA-6848	66.764	-30.84	PO-175/15	Foraminifera	14 845	190	17 229	16717–17791	Williams et al. (1995)
AA-11584	68.116	-31.43	91-K11A	Foraminifera	9975	100	10 942	10 585–11 239	Andrews et al. (1997)
CAMS-32047	68.100	-29.35	JM96-1207	Foraminifera	9800	60	10731	10 495–11 037	Jennings et al. (2002)
AA-29205	67.300	-30.97	JM96- 1214/2GC	Benthic foraminifera	11 380	80	12 786	12 601–13 009	Smith and Anderson (2000), Jennings et al. (2006)
AA-32045	67.047	-30.86	JM96- 1215/2GC	Benthic and planktic foraminifera	12 900	50	14 693	14 326–15 010	Smith and Anderson (2000), Jennings et al. (2006)
AA-23221	65.963	-30.63	JM96-1216/2- GC	Benthic foraminifera	14 550	150	16 862	16 423–17 296	Smith and Anderson (2000), Jennings et al. (2006)
AA-43116	68.093	-27.84	MD99-2317	Bryozoans	11 950	110	13405	13 122–13 717	Jennings et al. (2006)
AA-4666	67.410	-31.07	3	Foraminifera	9375	70	10 133	9818–10 424	Williams (1993), Miene et al. (1992)

 $<sup>^{*}</sup>$  Modelled median age derived from age-depth model (Davies et al., 2022; Hansen et al., 2022).



Figure 2. Representative boulder sample sites from outer Scoresby Sund (a, b, c), and the unnamed island near the terminus of Storstrømmen Glacier (d, e, f). (a) Sample 22-GRO-101, Uunarteq at the northern mouth of Scoresby Sund. (b) Sample 22GRO-131, Kap Brewster (Kangikajiip Appalia) at the southern mouth of Scoresby Sund. (c) Sample 22GRO-142, Rathbone Island, ~3 km to the east of the main coastline of Liverpool Land. (d) Sample 23DMH-29, from the prominent M1 moraine on the island at the terminus of Storstrømmen Glacier. (e) Sample 23DMH-33, adjacent to the historical moraine and modern ice margin. (f) Sample 23DMH-20, outboard of the moraine.

the fjord mouth is a large submarine moraine, Kap Brewster moraine (Fig. 3; Dowdeswell et al., 1994; Funder and Hansen, 1996).

Our study focuses on three presently ice-free sites on the outer coast of Scoresby Sund: Uunarteq on the northern mouth, Kap Brewster (Kangikajiip Appalia) on the southern mouth, and Rathbone Island, ~3 km to the east of the eastern coastline of Liverpool Land. At Uunarteq on the northern cape of Scoresby Sund, the local bedrock comprises Paleoproterozoic orthogneiss and granite (Kokfelt et al., 2023). Erratic boulders and cobbles of orthogneiss form a drift sheet over the local bedrock (Fig. 2a). At Kap Brewster on the southern cape of Scoresby Sund, the local bedrock comprises Paleogene basalts of the North Atlantic Igneous Province (Wager, 1947). The eastern margin of Kap Brewster is characterized by steep basalt cliffs that extend over 200 m a.s.l.. Erratic sandstone and orthogneiss boulders and cobbles (> 230 m a.s.l.) form a drift draped over the basaltic plateau above the cliffs (Fig. 2b; Håkansson et al., 2007a). At Rathbone Island, a thin drift of orthogneiss boulders and cobbles to at least 120 m a.s.l. overlie Paleozoic granodiorite and quartz diorite bedrock (Kokfelt et al., 2023; Fig. 2c).

Surface exposure <sup>10</sup>Be ages from the mouth of Scoresby Sund suggest the ice margin retreated west of Kap Brewster by  $\sim 14.5$  ka (Håkansson et al., 2007a). In Milne Land,  $\sim$  150 km west of Kap Brewster,  $^{10}$ Be exposure ages from the Milne Land stade moraines suggest ice retreated to southeastern Milne Land by  $\sim 11.4 \, \text{ka}$  (Levy et al., 2016). Notably, the Milne Land stade moraines have been mapped from Milne Land to Germania Land (Fig. 1), and <sup>10</sup>Be and radiocarbon ages constrain both local mountain glacier and GrIS retreat during the Younger Dryas (12.9-11.7 ka; Funder et al., 2011; Kelly et al., 2008; 2025; Levy et al., 2016). In northwestern Scoresby Sund, the Milne Land stade moraines grade into raised marine terraces (Funder, 1978), and radiocarbon dates from Kjove Land, suggested the outer Milne Land stade moraines were deposited just before  $\sim$  12.8 cal ka BP (Hall et al., 2008; Kelly et al., 2025). Additionally, radiocarbon dated shell samples from Schuchert Dal reveal the Milne Land stade moraines were deposited during the early Younger Dryas or late Allerød (Hall et al., 2010). The surface exposure ages in Scoresby Sund generally agree with radiocarbon ages from marine sediment cores (Dowdeswell et al., 1994; Marienfeld, 1991), bivalves (Funder, 1978, 1990; Hall et al., 2008), and plant macrofossils (Bennike et al., 1999; Hansen, 2001; Ingólfsson et al., 1994) which record ice retreat through the main trough of Scoresby Sund between 11.7 and 7.9 cal ka BP (Fig. 3).

#### 2.2 Storstrømmen Isstrom

Storstrømmen Isstrom is a major NEGIS outlet, and includes Kofoed-Hansen Bræ which drains to the northeast. and Storstrømmen Glacier which drains to the southeast (Fig. 4). The drainage basin (58 176 km<sup>2</sup>) of Storstrømmen Glacier contains enough ice to raise global sea level by 27 cm (Rignot et al., 2022). The southeastern lobe of Storstrømmen Glacier is a 23 km wide marine-terminating outlet glacier that drains into Borgfjorden of the Dove Bugt Embayment (Fig. 4). Storstrømmen is a surge glacier, with an estimated recurrence cycle of 50–70 years (Mouginot et al., 2018; Reeh et al., 1994). The terminus retreated 15 km between 1913 and 1950, remained stable between 1950 and 1978, and readvanced 8 km between 1978 and 1984 during a surge (Reeh et al., 1994). Grounding line retreat of 1.1 km from 2017–2021 has been attributed to increased surface ablation (Rignot et al., 2022). Recent observations suggest a possible surge onset projected to occur between 2027 and 2040 (Andersen et al., 2025).

At the terminus, Storstrømmen Glacier splits into two lobes that flow around an unnamed island where we collected samples for surface exposure dating. The western lobe merges with L. Bistrup Brae Glacier, and the eastern lobe flows directly into Borgfjorden. The unnamed island acts as

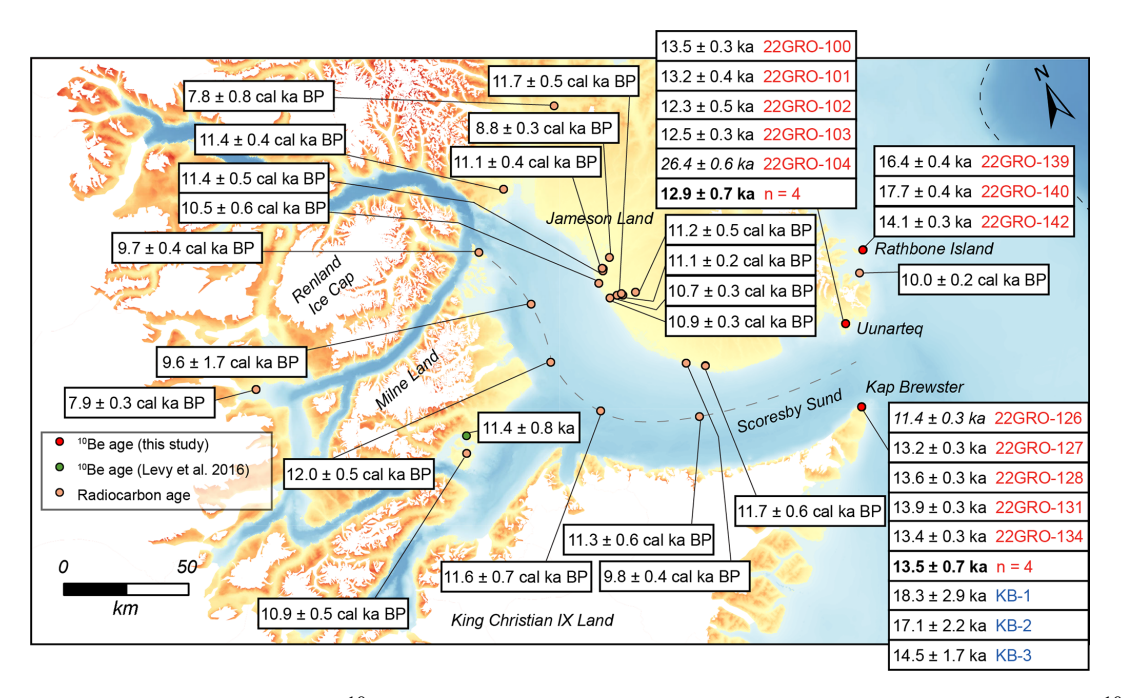


**Figure 3.** Scoresby Sund with new measured  $^{10}$ Be ages of boulders (red circles) with red sample names, and recalculated  $^{10}$ Be ages of Håkansson et al. (2007a) with blue sample names at Kap Brewster. All  $^{10}$ Be ages shown in kiloyears with  $1\sigma$  internal uncertainties. Mean  $^{10}$ Be ages from Uunarteq and Kap Brewster are shown in bold. Mean  $^{10}$ Be age (n = 8; green circle) from Milne Land (Levy et al., 2016). Radiocarbon ages (orange circles) are listed in Table 1.  $^{10}$ Be age outliers shown in italics. The grey dashed line denotes the flowline and  $^{10}$ Be and radiocarbon ages used to calculate average retreat rates. The maximum LGM extent is marked by the black dashed line, derived from Leger et al. (2024 and references therein).

a pinning point, stabilizing the present-day glacier (Reeh et al., 1994). The local bedrock of the island comprises basement Paleoproterozoic orthogneiss (Kokfelt et al., 2023) and is overlain by moraines and glacially transported erratics (Fig. 2d, e, f). At the southern end of the island, moraine deposits grade into a raised marine terrace at the local marine limit (28 m a.s.l.). This observation is consistent with the 28 m marine limit at Hellefjord in western Germania Land (Landvik, 1994; Weidick et al., 1996). Radiocarbon ages from marine bivalves in Neoglacial moraines indicate that Storstrømmen Glacier terminated inland from its present-day position between 5.4–1.2 cal ka BP, when a  $\sim 100$  km long sound formed between Kofoed-Hansen Bræ and Storstrømmen (Weidick et al., 1996). The ice margin of the unnamed island is surrounded by fresh (little weathered) "historical moraine" ridges and mark a late Neoglacial readvance that culminated  $\sim$  1850 (Weidick et al., 1996).

#### 3 Methods

## 3.1 Field methods

We collected samples from the mouth of Scoresby Sund and Rathbone Island during the boreal summer of 2022, and from the island at the terminus of Storstrømmen Glacier during the boreal summer of 2023. We sampled 13 boulders from

Scoresby Sund (Fig. 3), and 15 boulders and one bedrock surface from Storstrømmen (Fig. 5) for <sup>10</sup>Be analysis (Table 2). We targeted large (> 0.5 m diameter) boulders perched on bedrock or on well-developed moraines. The bedrock sample (23DMH-CR1-SURFACE) was collected from a surface with visible signs of glacial abrasion (e.g. glacial polish, striae). Four of the samples from Kap Brewster at the mouth of Scoresby Sund were collected from friable white sandstone boulders displaying exfoliation and weathering pits. We avoided sampling surfaces near the exfoliation or weathering pits. Three erratic boulder samples (22GRO-126, 22GRO-127, and 22GRO-128) from Kap Brewster were collected from the same boulders (KB-1, KB-2, and KB-3) as previously sampled by Håkansson et al. (2007a).

#### 3.2 Analytical methods

Whole rock samples from Scoresby Sund were crushed, sieved and processed to quartz purification at the University at Buffalo. Whole rock samples from Storstrømmen Glacier were crushed, sieved and processed to quartz purification at Lamont-Doherty Earth Observatory. All samples were then processed at Lamont-Doherty Earth Observatory via conventional <sup>10</sup>Be extraction methods (Schaefer et al., 2009). <sup>10</sup>Be/<sup>9</sup>Be ratios were measured at the Center for Accelerator Mass Spectrometry at Lawrence Livermore National Labo-

**Table 2.** Cosmogenic <sup>10</sup>Be concentrations and apparent exposure ages.

Sample name	Latitude (DD)	Longitude (DD)	Elevation (m a.s.l.)	Sample thickness (cm)	Topographic shielding	$^{10}$ Be conc. $(10^4 \text{ atoms g}^{-1})^a$	<sup>10</sup> Be age (ka) <sup>b,c,c</sup>
Rathbone							
Island							
22GRO-139	70.66612	-21.3985	118	3.00	1	$7.66 \pm 0.18$	$16.4 \pm 0.4 \ (0.6$
22GRO-140	70.66674	-21.3991	119	3.00	1	$8.25 \pm 0.20$	$17.7 \pm 0.4 \ (0.6$
22GRO-142	70.66599	-21.4040	97	2.5	1	$6.45 \pm 0.16$	$14.1 \pm 0.3 \ (0.5$
Most likely:							$14.1 \pm 0.3$
Uunarteq							
22GRO-100	70.44798	-21.8879	99	3.00	0.998	$6.19 \pm 0.15$	$13.6 \pm 0.3 (0.5)$
22GRO-101	70.44798	-21.8879	99	3.00	0.998	$6.04 \pm 0.17$	$13.2 \pm 0.4 \ (0.5)$
22GRO-102	70.44791	-21.8876	94	3.00	0.998	$5.56 \pm 0.23$	$12.3 \pm 0.5 \ (0.6)$
22GRO-103	70.44786	-21.8880	91	3.00	0.994	$5.64 \pm 0.14$	$12.5 \pm 0.3 \ (0.4)$
22GRO-104	70.44768	-21.8880	103	3.00	0.998	$12.20\pm0.26$	$26.4 \pm 0.6  (0.9)$
Kap Brewster (Ka	angikajiip Appalia)						
22GRO-126	70.15100	-22.0754	225	3.00	1	$5.99 \pm 0.17$	11.4 ± 0.3 (0.4
22GRO-127	70.15112	-22.0760	231	3.00	1	$6.97 \pm 0.18$	$13.2 \pm 0.3 \ (0.5$
22GRO-128	70.15112	-22.0761	233	3.00	1	$7.18 \pm 0.16$	$13.6 \pm 0.3 \ (0.5)$
22GRO-131	70.15077	-22.0766	227	3.00	1	$7.33 \pm 0.17$	$13.9 \pm 0.3 \ (0.5)$
22GRO-134	70.15005	-22.0756	230	3.00	1	$7.03 \pm 0.15$	$13.4 \pm 0.3 \ (0.5)$
Weighted mean (U	Junarteq and Kap Bro	ewster):					$13.2 \pm 0.7 \ (n = 8)$
Storstrømmen Gla	acier						
Outboard							
23DMH-CR1- SURFACE	76.87522	-22.3197	166	1.65	1	$5.63 \pm 0.15$	$11.5 \pm 0.3 (0.4)$
23DMH-18	76.87489	-22.3197	161	2.79	1	$5.93 \pm 0.16$	$12.3 \pm 0.3 (0.5)$
23DMH-20	76.87555	-22.3165	164	2.19	1	$4.25 \pm 0.15$	$8.7 \pm 0.3 \ (0.4)$
23DMH-21	76.87409	-22.3181	163	1.85	1	$4.33 \pm 0.09$	$8.9 \pm 0.2 (0.3)$
Weighted mean:							$8.8 \pm 0.3 \ (n=2)$
M1 moraine							
23DMH-22	76.85698	-22.2770	114	1.08	1	$4.48 \pm 0.11$	$9.6 \pm 0.2  (0.4)$
23DMH-23	76.85442	-22.2810	92	3.53	1	$3.82 \pm 0.19$	$8.6 \pm 0.4 \ (0.5)$
23DMH-24	76.85425	-22.2807	91	3.37	1	$3.72 \pm 0.08$	$8.4 \pm 0.2 \ (0.3)$
23DMH-25	76.85428	-22.2824	91	2.54	1	$3.84 \pm 0.12$	$8.6 \pm 0.3 \ (0.3$
23DMH-29	76.86870	-22.3197	152	3.67	1	$4.10 \pm 0.11$	$8.6 \pm 0.2 \ (0.3$
23DMH-30	76.86914	-22.3229	151	2.41	1	$4.19 \pm 0.11$	$8.7 \pm 0.2 \ (0.3)$
23DMH-31	76.87427	-22.3491	124	3.07	1	$3.92 \pm 0.09$	$8.5 \pm 0.2 \ (0.3)$
Weighted mean:							$8.6 \pm 0.3 \ (n = 6)$
Inboard							
23DMH-26	76.84808	-22.2882	38	2.39	1	$3.32 \pm 0.13$	$7.9 \pm 0.3 \ (0.4)$
23DMH-27	76.84876	-22.2989	90	2.40	1	$3.70 \pm 0.09$	$8.3 \pm 0.2 \ (0.3$
23DMH-28	76.85110	-22.3069	109	1.07	1	$3.80 \pm 0.09$	$8.2 \pm 0.2 \ (0.3$
23DMH-32	76.88953	-22.3271	127	2.01	1	$3.80 \pm 0.10$	$8.1 \pm 0.2 \ (0.3)$
23DMH-33	76.89405	-22.3273	125	2.22	1	$3.72 \pm 0.09$	$8.0 \pm 0.2 \ (0.3$
Weighted mean:							$8.1 \pm 0.3 \ (n = 5)$

<sup>&</sup>lt;sup>a</sup> Samples normalized to the 07KNSTD standard of Nishiizumi et al. (2007). <sup>b</sup> Exposure ages calculated using the CRONUS-Earth calculator (https://hess.ess.washington.edu/, last access: 9 February 2025), using the Lm scaling scheme (Lal, 1991; Stone, 2000) and the Arctic production rate (Young, et al., 2013a). <sup>c</sup> Both internal and external uncertainties shown at the 1 $\sigma$  level. Internal uncertainties are analytical uncertainties only, and external uncertainties (given in parentheses) are absolute uncertainties and include production rate and scaling errors. <sup>d</sup> The weighted mean for each site includes the propagation of a 3.7 % production rate uncertainty (Young et al., 2013a). Outliers in italics are excluded from the weighted mean age.

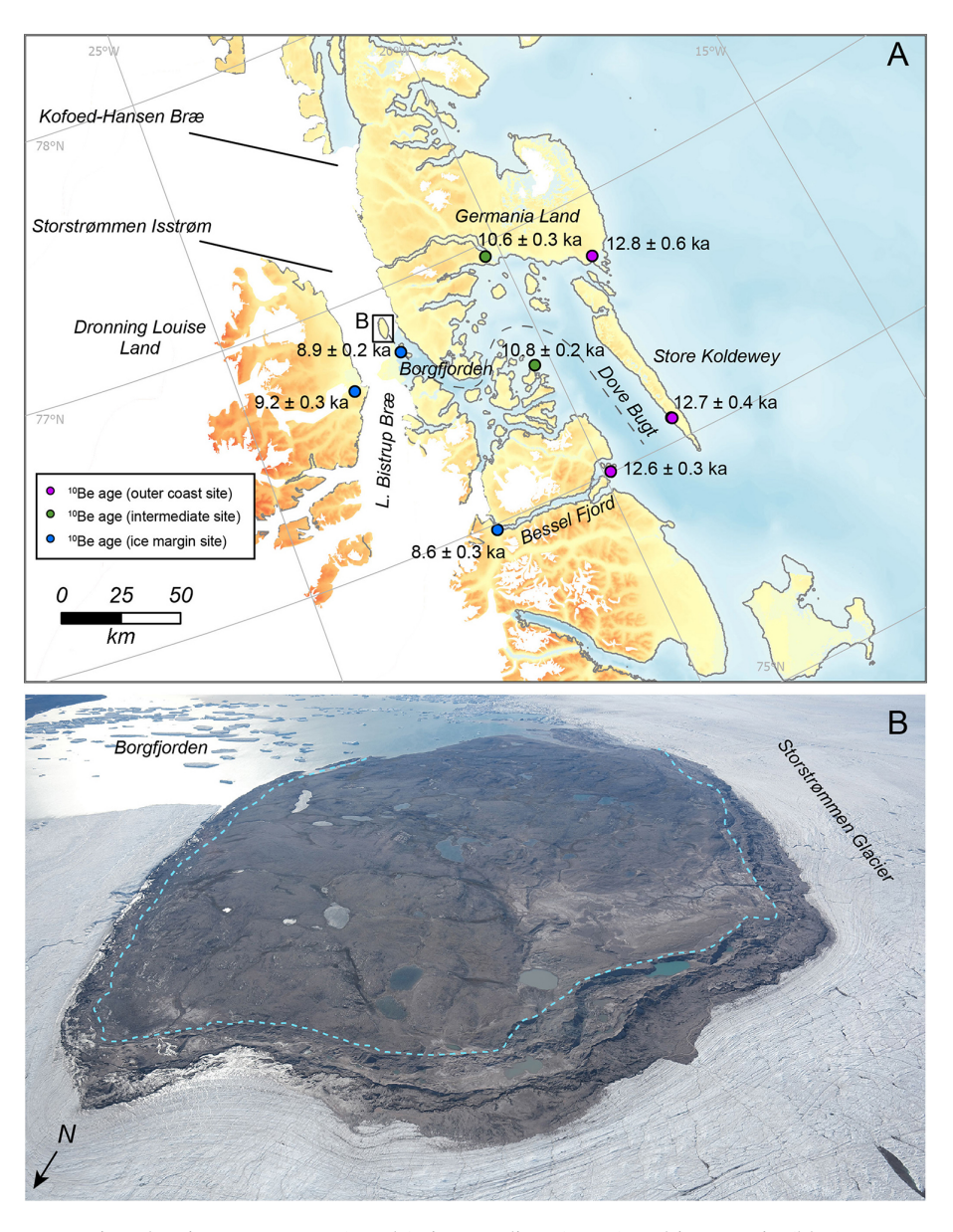


**Figure 4.** (**A**) Dove Bugt region showing outer coast (purple), intermediate (green) and ice margin (blue) exposure ages from Larsen et al. (2022). The outer coast mean ages are 12.8 ka (n = 1), 12.7 ka (n = 3), 12.6 ka (n = 3). The intermediate mean ages are 10.8 ka (n = 3), 10.6 ka (n = 4). The ice margin mean ages are 9.1 ka (n = 3), 8.9 ka (n = 3), 8.6 ka (n = 6). Black inset shows the location of Storstrømmen Glacier terminus in aerial photo (**B**) and in Fig. 5. The grey dashed line denotes the flowline used to calculate average retreat rates. The mean 10 Be ages used to calculate average retreat rates are 12.7, 10.8, and 8.9 ka. (**B**) View looking south at the Storstrømmen Glacier terminus showing the historical moraine (blue dashed line) and modern ice margin.

ratory, and normalized to the 07KNSTD standard of Nishiizumi et al. (2007) with a nominal ratio of  $2.85 \times 10^{-12}$ . Blank corrections to measured  $^9\mathrm{Be/^{10}Be}$  ratios amounted to <2%, and process blanks range from 6200–11 855  $^{10}\mathrm{Be}$  atoms (Table S2). Final errors in  $^{10}\mathrm{Be}$  concentrations are obtained by quadrature addition of the final accelerator mass spectrometry analytical error, and a 1% error in Be spike concentration. We calculated our new surface exposure ages and recalculated previously reported ages using version 3 of the CRONUS-Earth calculator (http://hess.ess.washington.edu/, last access: 9 February 2025; Balco et al., 2008) using the Lm scaling scheme (Lal, 1991; Stone, 2000) and the Arctic production rate (Young, et al., 2013a; Table S1 in the Supplement). We note that using the St scaling scheme results in almost identical ages for our samples, while ages derived using the LSDn scaling scheme differ by less than 120 years, and thus do not affect our interpretations. Four samples are quartz sandstone boulders collected from Kap Brewster (22GRO-126, 22GRO-127, 22GRO-128, 22GRO-131) and we use a density of  $2.4 \,\mathrm{g \, cm^{-3}}$ . All other samples are crystalline boulders or bedrock (e.g., orthogneiss, granodiorite) and we use a density of 2.65 g cm<sup>-3</sup>. Unless otherwise noted, all radiocarbon ages (reported as: cal ka BP) mentioned in the text are recalculated using CALIB 8.2 (Stuiver and Reimer, 1993); http://calib.org/calib/calib.html, last access: 18 April 2025), and the IntCal20 calibration curve (Reimer et al., 2020) for terrestrial samples, or the Marine 20 calibration curve (Heaton et al., 2020) for marine samples (Tables 1, S3). For marine samples, marine reservoir corrections were calculated using the Marine Reservoir Correction Database (http://calib.org/marine/, last access: 18 April 2025) (Reimer and Reimer, 2001). Each site uses an average  $\Delta R$  value based on water depth, distance to coast, and where possible, species that are most representative of the study site, as suggested in Pearce et al. (2023).

#### 4 Results

## 4.1 Scoresby Sund

The 13 erratic boulder samples from the outer coast of the Scoresby Sund region produce <sup>10</sup>Be ages that range from  $11.4 \pm 0.3 - 26.4 \pm 0.6$  ka (Figs. 3,6). On Rathbone Island, east of Scoresby Sund, three erratic boulders were sampled between 97 and 118 m elevation and produce exposure ages of  $14.1 \pm 0.3$  ka (22GRO-142),  $16.4 \pm 0.4$  ka (22GRO-139), and  $17.7 \pm 0.4 \text{ ka}$  (22GRO-140). At Uunarteq located at the northern mouth of Scoresby Sund, five erratic boulders sampled between 91 and 103 m elevation produce  $^{10}$ Be ages that range from  $12.3 \pm 0.5$ -26.4 ± 0.6 ka. At Kap Brewster (Kangikajik) located at the southern mouth of Scoresby Sund, five erratic boulders sampled between 225 and 233 m elevation produce <sup>10</sup>Be ages that range from  $11.4 \pm 0.3$  to  $13.9 \pm 0.3$  ka. The  $^{10}$ Be ages from samples 22GRO-126, 22GRO-127, and 22GRO-128 are  $11.4 \pm 0.3$  ka,  $13.2 \pm 0.6$  ka, and  $13.6 \pm 0.3$  ka, respectively; these samples were collected from the same boulders as samples KB-1, KB-2, and KB-3 from Håkansson et al. (2007a), which yield recalculated ages of  $18.3 \pm 2.9$  ka,  $17.2 \pm 2.2$  ka, and  $14.5 \pm 1.7$  ka. The large difference in ages is outside the  $1\sigma$  error range, and may be attributed to analytical errors. After excluding one older outlier (26.4  $\pm$  0.6 ka) from Uunarteq, and a younger outlier from Kap Brewster  $(11.4 \pm 0.3 \,\mathrm{ka})$ , the mean age from the two sites at the mouth of Scoresby Sund is  $13.2 \pm 0.7$  ka (n = 8; Table 2).

### 4.2 Storstrømmen Glacier

The 15 erratic boulder samples from the unnamed island at the Storstrømmen Glacier terminus produce  $^{10}$ Be ages that range from  $7.9 \pm 0.3 - 12.3 \pm 0.3$  ka (Figs. 5, 6). Exclud-

ing two outliers (23DMH-18, 23DMH-22) the mean age of the boulders on the island is  $8.4 \pm 0.4$  ka (n = 13; Table 2). Of these, seven samples were collected from boulders on a prominent moraine (M1 moraine) deposited by the western lobe that extends  $\sim 5 \, \text{km}$  through the island, and produce  $^{10}$ Be ages of  $9.6 \pm 0.2$ ,  $8.6 \pm 0.4$ ,  $8.4 \pm 0.2$ ,  $8.6 \pm 0.3$ ,  $8.6 \pm 0.2$ ,  $8.7 \pm 0.2$ , and  $8.5 \pm 0.2$  ka. The mean age for the M1 moraine is  $8.6 \pm 0.3$  ka (n = 6), excluding sample 23DMH-22 ( $9.6 \pm 0.2 \,\mathrm{ka}$ ), which was identified as an outlier (Fig. 6).  $^{10}$ Be ages from three boulders  $\sim 500$  m north and outboard of the moraine are  $8.7 \pm 0.3$ ,  $8.9 \pm 0.2$ , and  $12.3 \pm 0.3$  ka. The  $12.3 \pm 0.3$  ka sample (23DMH-18) outboard of the M1 moraine was identified as an outlier as it falls outside of the  $2\sigma$  range of the mean age of the boulders on the island. The one bedrock surface,  $\sim 500$  m north of the moraine and in close proximity to 23DMH-18, produced a  $^{10}$ Be age of 11.5  $\pm$  0.3 ka (23DMH-CR1-SURFACE). The bedrock surface likely has inherited <sup>10</sup>Be and was not used to determine deglacial history.

On the southeastern side of the island,  $^{10}$ Be ages from three boulders close to the raised marine terrace are  $7.9\pm0.3$ ,  $8.3\pm0.2$ , and  $8.2\pm0.2$  ka, and are inboard of the M1 moraine. On the northern margin of the island,  $^{10}$ Be ages from two boulders adjacent to the historical moraine and modern ice margin are  $8.1\pm0.2$  ka (23DMH-32) and  $8.0\pm0.2$  ka (23DMH-33). These boulders were deposited by the eastern lobe.

## 5 Discussion

#### 5.1 Glacier evolution in Scoresby Sund

The  $^{10}$ Be exposure ages from Rathbone Island provide new minimum constraints on the retreat of the GrIS off the coast of Liverpool Land at  $14.1 \pm 0.3$  ka, and record one of the earliest terrestrial deglaciation events in Greenland. Our mean  $^{10}$ Be age of  $13.2 \pm 0.7$  ka (n=8) from the north and south sides of the mouth of Scoresby Sund is consistent with the minimum  $^{10}$ Be exposure age from Kap Brewster reported by Håkansson et al. (2007a) of  $14.5 \pm 1.7$  ka, and provides a minimum constraint on ice margin retreat past the mouth of Scoresby Sund (Fig. 6). Based on our age constraints at the mouth of Scoresby Sund, we infer the depositional age of the Kap Brewster submarine moraine to correspond with our mean age of  $\sim 13.2$  ka.

At sites ( $\geq$  300 km) north of Scoresby Sund, the outer coast deglaciated between 12.8  $\pm$  0.6 and 11.5  $\pm$  0.2 ka (Larsen et al., 2022). This retreat chronology is consistent with mountain glacier retreat between  $\sim$  12.8 and 11.7 ka from Milne Land, Kjove Land, Gurreholm Dal and Schuchert Dal derived from <sup>10</sup>Be and radiocarbon ages (Hall et al., 2008; 2010; Kelly et al., 2008; 2025; Levy et al., 2016). We suggest the earlier onset of deglaciation at the outer coast of the Scoresby Sund region may be related to the closer proximity of our dated sites to the edge of the continen-

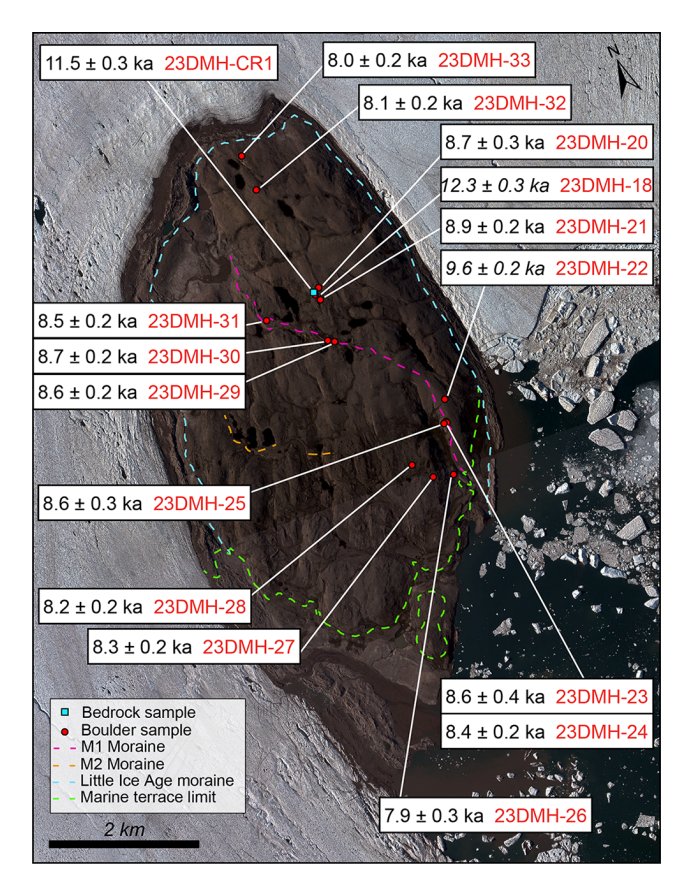


**Figure 5.** Map of Storstrømmen Glacier terminus with extent of Little Ice Age moraine (blue dashes) and raised marine terrace limit (green dashes). The M1 moraine (magenta) deposited by the western lobe, grades into the marine terrace at 28 m elevation. Measured  $^{10}$ Be ages of boulders (red circles) and bedrock (blue square) are shown in kiloyears (ka) with  $1\sigma$  internal uncertainties.  $^{10}$ Be age outliers shown in italics. Satellite image from WorldView-2 (© Maxar, 2021).

tal shelf than other parts of East Greenland. This interpretation is further supported by deglaciation chronologies before 13.4 cal ka BP, and 13.3 cal ka BP on the northeast Greenland shelf (Davies et al., 2022; Hansen et al., 2022).

The timing of retreat at Rathbone Island at  $\sim$  14.1 ka, to the mouth of Scoresby Sund at  $\sim$  13.2 ka, coincides with the Bølling-Allerød warm period (14.7–12.9 ka, Rasmussen et al., 2006), suggesting widespread retreat of the GrIS across the eastern continental shelf. Retreat from across the northeast Greenland shelf between 16.6 and 13.4 cal ka BP (Davies et al., 2022; López-Quirós et al., 2024), coincides broadly with Meltwater Pulse 1A, a period of rapid sea level rise between 14.6 and 14.3 ka (Deschamps et al., 2012; Hanebuth et al., 2000). Alongside our  $^{10}$ Be ages from Rathbone Island, we suggest that ice margin retreat across the East Greenland shelf may have been influenced, in part, by enhanced sensitivity to abrupt global sea-level rise at this time. The retreat of ice in the Scoresby Sund region was likely

attributed to the influx of warm Atlantic water that flowed onto the East Greenland continental shelf, perhaps related to the Bølling-Allerød warm period (Hansen et al., 2022). The inflow of Atlantic water beneath fresher and colder polar surface water has been inferred by high abundances of *Cassidulina neoteretis* (Foraminifera) in marine sediment cores, a species typically found in Atlantic sourced subsurface waters (Cage et al., 2021; Consolaro et al., 2018). In southeast Greenland, the high abundance of *C. neoteretis* in shelf cores—also suggests the advection of Atlantic water into the Kangerlussuaq Trough drove basal melt and retreat during the Bølling-Allerød and the Younger Dryas (Jennings et al., 2006).

Our retreat chronology, and previously published  $^{10}$ Be and radiocarbon ages in Scoresby Sund, suggest ice in the main fjord basin of Scoresby Sund retreated from the mouth of Scoresby Sund at  $\sim 13.2\,\mathrm{ka}$  to Renland by 9.7 cal ka BP (Funder, 1978), and using the flowline in Fig. 3, we calculate an average retreat rate of  $\sim 43\,\mathrm{m\,yr^{-1}}$ . In southern Scoresby Sund, ice retreated  $\sim 150\,\mathrm{km}$  from the mouth to the southern end of Milne Land by  $\sim 11.4\,\mathrm{ka}$  (Levy et al., 2016) at an average retreat rate of  $\sim 83\,\mathrm{m\,yr^{-1}}$ .

# 5.2 Glacier evolution in the Dove Bugt region

Our mean  $^{10}$ Be age of  $8.6 \pm 0.3$  ka (n = 6) from the prominent M1 moraine at Storstrømmen Glacier record the conclusion of a stillstand or advance near the modern ice margin (Fig. 6). This age is consistent with the <sup>10</sup>Be retreat chronology at Bræ Øerne of  $8.9 \pm 0.2$  ka (Larsen et al., 2022),  $\sim$  14 km south of Storstrømmen Glacier (Fig. 4). We suggest Storstrømmen Glacier comprised two expanded ice lobes around the eastern and western margins of the unnamed island. As the glacier retreated, boulders and moraines were deposited between  $\sim$  8.6 and 8.0 ka (Figs. 2, 5). The western ice lobe deposited the prominent M1 moraine in the middle of the island and all the boulders inboard (west) of the moraine. As the glacier retreated the western lobe wrapped around the southern end of the island depositing the M2 moraine. Two lakes  $\sim 1.5 \, \text{km}$  south of sample 23DMH-31 on the M2 moraine are dammed at their southern end, and we interpret these to be moraine dammed lakes that formed as the western lobe retreated (Fig. 5). The eastern lobe ice likely retreated beyond the historical moraine, and present ice margin at  $\sim$  8 ka.

The 28 m marine limit at the terminus of Storstrømmen (Weidick et al., 1996) is dated to an estimated age of  $\sim 8 \, \mathrm{cal} \, \mathrm{ka} \, \mathrm{BP}$  with marine bivalves (Landvik, 1994; Fig. 7). Our exposure ages from the unnamed island are consistent with the radiocarbon ages of the raised marine sediments. Also, our ice margin retreat history is in agreement with deglaciation of inner Kejser Franz Joseph Fjord and Nordfjord,  $\sim 360 \, \mathrm{km}$  south of Storstrømmen, constrained by radiocarbon ages of 8.5 and 7.5 cal ka BP, respectively (Olsen et al., 2022).

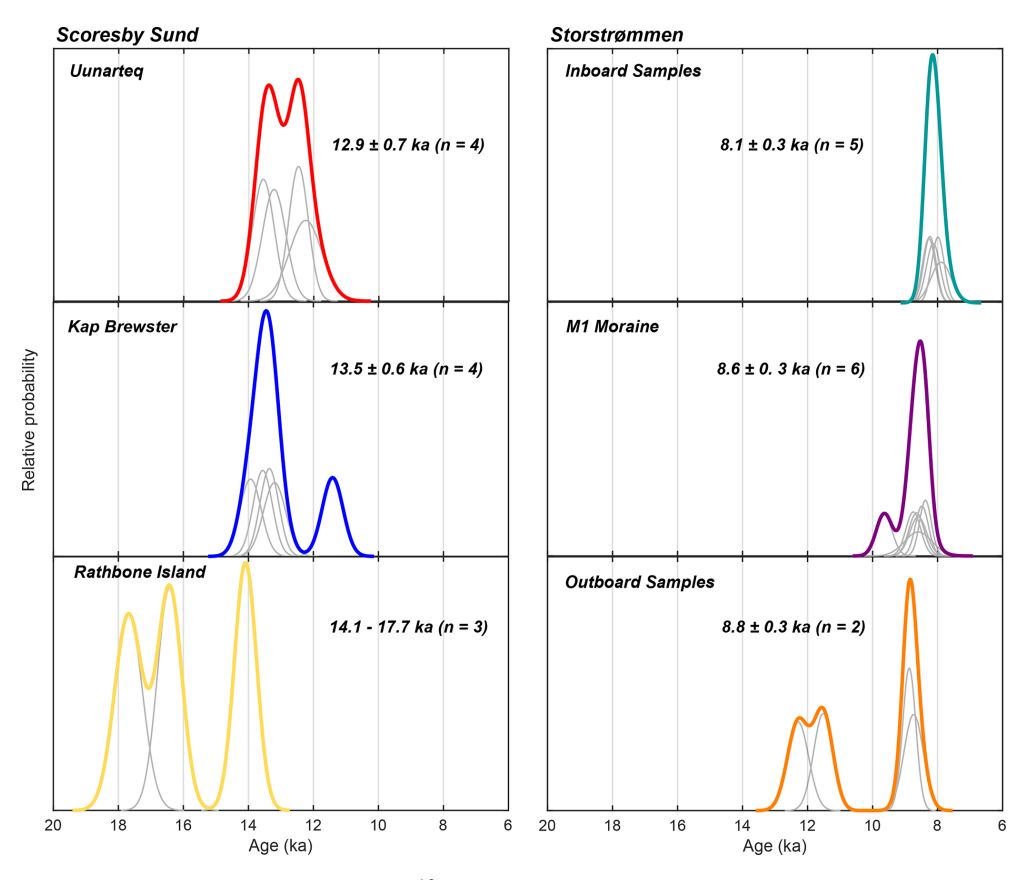


**Figure 6.** Camel plots (normal kernel density function) for <sup>10</sup>Be exposure ages Uunarteq, Kap Brewster and Rathbone Island near the outer coast of Scoresby Sund, and samples from the M1 moraine, and inboard and outboard of the M1 moraine at the terminus of the Storstrømmen Glacier. Colored camel plots show the relative probability for all <sup>10</sup>Be ages at each site.

Our  $^{10}$ Be ages from the M1 moraine at  $\sim 8.6$  ka to near the modern ice margin  $\sim 8$  ka suggests an ice margin stillstand or slowdown of ice retreat, broadly consistent with the abrupt 8.2 ka cooling event (Alley et al., 1997). The formation of the M1 moraine  $(8.6 \pm 0.3 \,\mathrm{ka})$  could be related to a period of ice margin stagnation in response to local cooling or localized dynamics unrelated to climate at this time. In West Greenland, surface exposure dating of moraine systems record the ice margin responded directly to the 9.3 and 8.2 ka cooling events (Young et al., 2013b). These observations support regional cooling across Greenland during this interval. However, considering present-day Storstrømmen is a surge glacier (Andersen et al., 2025; Mouginot et al., 2018; Reeh et al., 1994), an alternative explanation is that the moraine records past surge dynamics, similar to modernday processes. Another alternative explanation is that the ice margin was pinned to the island  $\sim 8.6$  ka, slowing ice retreat during this time, independent of any climate event.

The response of the GrIS to climate variability is strongly influenced by ice flux (Young, et al., 2013b). In low ice flux glaciers, such as Storstrømmen, mass balance change driven by regional cooling (i.e., reduced summer ablation), may occur slowly resulting in a subtle response or stillstand. In con-

trast, the response to high flux glaciers, such as Jakobshavn Isbræ in West Greenland, to such cooling may occur relatively quickly resulting in an ice sheet advance (Young, et al., 2013b). For example, at Jakobshavn Isbræ, a high flux environment was observed between ~8.5–8.1 ka, directly depositing moraines during the 8.2 ka event (Young et al., 2013b). Our observations in northeast Greenland, are consistent with patterns observed in West Greenland (Young, et al., 2013b; Young et al., 2011), suggesting that marine-terminating glaciers show high sensitivity to abrupt warming and cooling on centennial timescales. In contrast, land-terminating glaciers in Greenland are less sensitive to abrupt climate change (Long et al., 2006; Young et al., 2011).

We estimate a minimum average retreat rate of  $\sim 28\,\mathrm{m\,yr^{-1}}$  for the outer coast near Store Koldewey at  $\sim 12.7\,\mathrm{ka}$  (Larsen et al., 2022) to within  $\sim 3\,\mathrm{km}$  of the modern ice margin by  $\sim 8.6\,\mathrm{ka}$ . The average retreat rate of Storstrømmen during the last deglaciation is an order of magnitude lower than the observed grounding line retreat of 1.1 km at a rate of 250–380 m yr<sup>-1</sup> between 2017 and 2021, attributed to surface ablation (Rignot et al., 2022). However, the modern retreat follows a surge event between 1978 and 1984 (Reeh et al., 1994), and present surge behavior may be

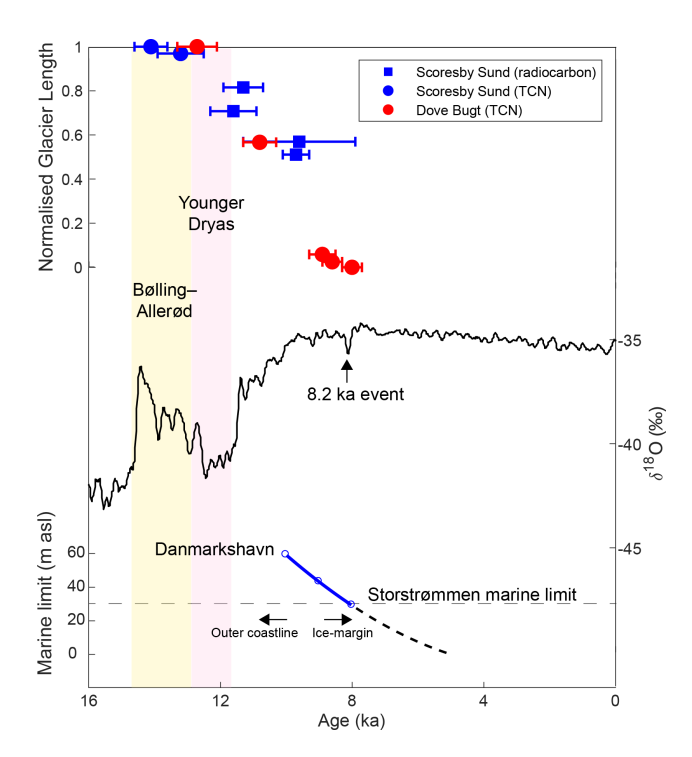


**Figure 7.** Ice margin retreat from Scoresby Sund and the Dove Bugt region.  $\delta^{18}$ O record of the North Greenland Ice core Project (NGRIP members, 2004). Marine limit curve for the Dove Bugt region derived from Weidick et al. (1996). Normalized glacier length includes published radiocarbon ages from Scoresby Sund (Dowdeswell et al., 1994; Funder, 1978; Marienfeld, 1991) and published terrestrial cosmogenic nuclide  $^{10}$ Be ages from the Dove Bugt embayment (Larsen et al. 2022).

related glacier instability. Therefore, direct comparisons between Holocene and modern retreat rates at Storstrømmen require caution. Additionally, differences in temporal resolution, the drainage system, and in external forcing such as ablation rates and ocean temperatures must be considered when comparing retreat rates across different timescales.

## 5.3 Rates of marine-terminating glacier retreat

As ice retreated westward out of the Greenland Sea, minimum average retreat rates of ice streams from the middle of the continental shelf to the outer coast of northeast Greenland were 96 m yr $^{-1}$  from Foster Bugt to the mouth of Kejser Franz Joseph Fjord (Olsen et al., 2022). At the Store Koldewey Trough, located east of Store Koldewey Island and the Dove Bugt embayment, retreat rates ranged between 80–400 m yr $^{-1}$  (Olsen et al., 2020). In contrast, our minimum average retreat rates observed at Scoresby Sund ( $\sim 43~{\rm m\,yr}^{-1}$ ) and Storstrømmen Glacier ( $\sim 28~{\rm m\,yr}^{-1}$ ) are consistent with broader estimates for marine-terminating glaciers in East Greenland fjords, which range between 10 and 80 m yr $^{-1}$  (Dyke et al., 2014; Hughes et al., 2012).

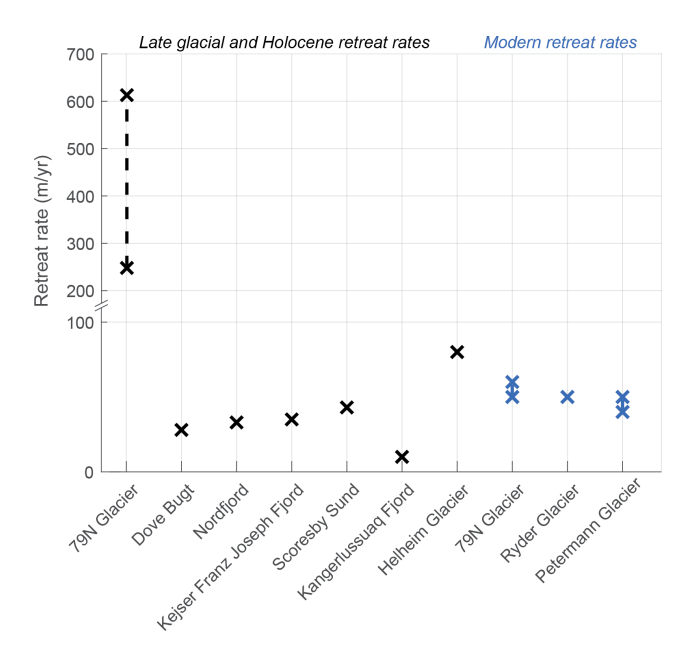


**Figure 8.** Rates of ice margin retreat (m yr<sup>-1</sup>) for marineterminating outlet glaciers in East Greenland during the late glacial and Holocene, compared with modern subglacial melt rates from 79° N Glacier, Ryder Glacier and Petermann Glacier (Wilson et al., 2017).

We summarize the late glacial and Holocene rates of retreat in East Greenland in Fig. 8. For comparison, retreat rates include 33 m yr<sup>-1</sup> at Nordfjord, and 35 m yr<sup>-1</sup> at Kejser Franz Joseph Fjord (Olsen et al., 2022);  $\sim 10 \,\mathrm{m\,yr^{-1}}$  at Kangerlussuaq Fjord (Dyke et al., 2014); and  $\sim 80 \,\mathrm{m\,yr^{-1}}$  at Helheim Glacier (Hughes et al., 2012). Rapid retreat rates of 79° N Glacier within Nioghalvfjerdsfjorden after 10 ka range between 248.5 and 613 m yr<sup>-1</sup> record some of the highest retreat rates in both Greenland and Antarctica (Roberts et al., 2024). Our retreat rates at Scoresby Sund ( $\sim 43 \,\mathrm{m\,yr^{-1}}$ ) are comparable to retreat rates for the entire central East Greenland region  $(35 \pm 23 \,\mathrm{m\,yr^{-1}})$ , while our retreat rates at Dove Bugt ( $\sim 28 \,\mathrm{m\,yr^{-1}}$ ) are lower than for the entire Northeast Greenland region  $(44 \pm 10 \,\mathrm{m\,yr^{-1}})$  that were estimated using transects across isochrones (Leger et al., 2024). In West Greenland, Young et al. (2011) estimated an average retreat rate of  $\sim 100 \,\mathrm{m\,yr}^{-1}$  for Jakobshavn Isbræ between 8–7.5 ka. The thickest and fastest moving parts of Greenland's largest present-day ice streams correspond to the contemporary submarine melt rates at 79° N (50–60 m yr<sup>-1</sup>) in northeastern Greenland, and Petermann Glacier (40–50 m yr<sup>-1</sup>) and Ryder Glacier (50 m yr<sup>-1</sup>) in northwestern Greenland (Wilson et al., 2017). These modern rates are comparable to late glacial and Holocene retreat rates observed in East Greenland (Fig. 8).

Fast flowing glaciers that lack topographic pinning points that enhance ice stability (i.e., islands, upward sloping beds) are particularly susceptible to rapid retreat (Mouginot et al.,

2015). Modern ice flow rates at Jakobshavn (11–17 km yr<sup>-1</sup>; Joughin et al., 2014), Helheim (5–11 km yr<sup>-1</sup>; Bevan et al., 2012) and 79° N (1.4 km yr<sup>-1</sup>; Vijay et al., 2019), all reflect fast flowing outlet glaciers of the GrIS with large volumes of ice discharge. By comparison, Storstrømmen Glacier has flow speeds of 0.19 km yr<sup>-1</sup> (Vijay et al., 2019), an order of magnitude slower than the fastest flowing glaciers of Greenland. This observation is also reflected in late glacial and Holocene retreat patterns in East Greenland fjords. With the exception of 79° N Glacier, retreat rates observed within the East Greenland fjords during the late glacial and Holocene were generally lower than those observed from the middle shelf to the outer coast. This pattern suggests a shift from large ice streams to topographically controlled retreat within fjord systems.

Numerical simulations from southwestern Greenland suggested ice calving within fjord systems significantly impact enhanced ice discharge at the terminus of outlet glaciers during the early Holocene (Cuzzone et al., 2022). Therefore, future ice sheet modeling, benchmarked against geologic constraints of past East GrIS change (e.g., Briner et al., 2020) could greatly improve estimations of ice mass loss, rates or retreat, and associated processes from marine-terminating outlet glaciers across Greenland.

#### 6 Conclusion

We report new <sup>10</sup>Be ages from Scoresby Sund on the outer coast in central east Greenland, and from near the modern ice margin of Storstrømmen Glacier in northeast Greenland. These new exposure ages provide direct constraints of the late glacial and early Holocene timing of ice retreat westward out of the Greenland Sea, within the present-day coastline, and within the modern ice margin. Our key findings include:

- Ice retreated from Rathbone Island, east of Scoresby Sund, by  $\sim$  14.1 ka, recording one of the earliest known terrestrial deglaciation events in Greenland. Our  $^{10}{\rm Be}$  ages support the idea that ice margin retreat across the East Greenland shelf was perhaps in response to enhanced sensitivity of abrupt global sea-level rise.
- Ice retreated from the mouth of Scoresby Sund at  $\sim 13.2\,\mathrm{ka}$  during the Bølling-Allerød warm period, perhaps related to an influx of warm Atlantic water that flowed onto the East Greenland continental shelf (Hansen et al., 2022).
- Storstrømmen Glacier reached  $\sim 3$  km from the modern ice margin at  $\sim 8.6$  ka and reached the modern margin  $\sim 8$  ka. The ice margin slowed or reached a still-stand between 8.6-8.0 ka. In low ice flux environments, such as Storstrømmen, mass balance change is driven by regional cooling and may occur slowly resulting in a subtle response or stillstand. These observations suggest that marine-terminating sectors of the eastern GrIS

- may be highly sensitive to abrupt warming and cooling events on centennial timescales.
- Average rates of marine-terminating glacier retreat at Scoresby Sund were ~43 m yr<sup>-1</sup> between ~13.2 and 9.7 ka. Average rates of marine-terminating glacier retreat in the Dove Bugt region were ~28 m yr<sup>-1</sup> between ~12.7 and ~8.6 ka. The rates of late glacial and Holocene retreat at Scoresby Sund, and Storstrømmen Glacier are within previously reported estimates of marine-terminating outlet glacier retreat across eastern Greenland fjords (10−80 m yr<sup>-1</sup>; Dyke et al., 2014; Hughes et al., 2012). These retreat rates are also comparable to modern retreat rates observed at the largest ice streams in northeastern (50−60 m yr<sup>-1</sup>), and northwestern Greenland (40−50 m yr<sup>-1</sup>; Wilson et al., 2017).
- The exposure ages from both regions of East Greenland provide robust constraints for ice sheet models, improving the accuracy of simulating past GrIS change. These data refine our understanding of the timing, rates and mechanisms of ice sheet retreat during the last deglaciation, and provide important context for understanding contemporary rates of ice mass loss from the GrIS.

**Data availability.** All data described in the paper are included in the Supplement. Data from surface samples are archived on the ICE-D Greenland database: https://version2.ice-d.org/greenland/publication/1381/ (last access: 3 November 2025).

**Supplement.** The supplement related to this article is available online at https://doi.org/10.5194/cp-21-1-2025-supplement.

**Author contributions.** NEY, JPB and JMS designed the study. NEY, AB-K, KKP, CKW-G, BG, JPB and JMS conducted fieldwork and sample collection. JTHA and KKP processed the samples and JTHA conducted sample analysis and initial interpretations. JTHA prepared the manuscript with contributions from all authors.

**Competing interests.** The contact author has declared that none of the authors has any competing interests.

**Disclaimer.** Any use of trade, firm, or product names is for descriptive purposes only and does not imply endorsement by the U.S. Government.

Publisher's note: Copernicus Publications remains neutral with regard to jurisdictional claims made in the text, published maps, institutional affiliations, or any other geographical representation in this paper. While Copernicus Publications makes every effort to include appropriate place names, the final responsibility lies with the authors. Views expressed in the text are those of the authors and do not necessarily reflect the views of the publisher.

**Acknowledgements.** We thank Volcano Heli for field support; Liza Wilson for assistance in the field; and Roseanne Schwartz, Jean Hanley, Kylie Seward, and Maya Lasker for laboratory assistance. Alan Hidy and Tyler Anderson are thanked for AMS measurements at Lawrence Livermore National Laboratory. The USGS internal reviewers are thanked for their feedback.

**Financial support.** The research was supported by the National Science Foundation Office of Polar Programs (awards no. 2105908 to NEY and JMS; award no. 2106971 to JPB).

**Review statement.** This paper was edited by Stephen Obrochta and reviewed by two anonymous referees.

#### References

- Alley, R. B., Mayewski, P. A., Sowers, T., Stuiver, M., Taylor, K. C., and Clark, P. U.: Holocene climatic instability: A prominent, widespread event 8200 yr ago, Geology, 25, 483, https://doi.org/10.1130/0091-7613(1997)025<0483:HCIAPW>2.3.CO;2, 1997.
- An, L., Rignot, E., Wood, M., Willis, J. K., Mouginot, J., Khan, S. A.: Ocean melting of the Zachariae Isstrøm and Nioghalvfjerdsfjorden glaciers, northeast Greenland, Proceedings of the National Academy of Sciences, 118, e2015483118, https://doi.org/10.1073/pnas.2015483118, 2021.
- Andersen, J. K., Meyer, R. P., Huiban, F. S., Dømgaard, M. L., Millan, R., and Bjørk, A. A.: Brief communication: Storstrømmen Glacier, northeastern Greenland, primed for end-of-decade surge, The Cryosphere, 19, 1717–1724, https://doi.org/10.5194/tc-19-1717-2025, 2025.
- Andrews, J. T., Smith, L. M., Preston, R., Cooper, T., and Jennings, A. E.: Spatial and temporal patterns of iceberg rafting (IRD) along the East Greenland margin, ca. 68 N, over the last 14 cal. ka., Journal of Quaternary Science: Published for the Quaternary Research Association, 12, 1–13, https://doi.org/10.1002/(SICI)1099-1417(199701/02)12:1<1::AID-JQS288>3.0.CO;2-T, 1997.
- Arndt, J. E., Jokat, W., Dorschel, B., Myklebust, R., Dowdeswell, J. A., and Evans, J.: A new bathymetry of the Northeast Greenland continental shelf: Constraints on glacial and other processes, Geochemistry, Geophysics, Geosystems, 16, 3733–3753, https://doi.org/10.1002/2015GC005931, 2015.
- Arndt, J. E., Jokat, W., and Dorschel, B.: The last glaciation and deglaciation of the Northeast Greenland continental shelf revealed by hydro-acoustic data. Quaternary Science Reviews, 160, 45–56, https://doi.org/10.1016/j.quascirev.2017.01.018, 2017.
- Balco, G., Stone, J. O., Lifton, N. A., and Dunai, T. J.: A complete and easily accessible means of calculating surface exposure ages or erosion rates from <sup>10</sup>Be and <sup>26</sup>Al measurements, Quaternary Geochronology, 3, 174–195, https://doi.org/10.1016/j.quageo.2007.12.001, 2008.
- Bennike, O., Bjorck, S., Bocher, J., Hansen, L., Heinemeier, J., and Wohlfarth, B.: Early Holocene Plant and Animal Re-

- mains from North-East Greenland, Journal of Biogeography, 26, https://doi.org/10.1046/j.1365-2699.1999.t01-1-00315.x, 1999.
- Bennike, O., and Weidick, A.: Late Quaternary history around Nioghalvfjerdsfjorden and Jøkelbugten, North-East Greenland, Boreas, 30, 300–9483, https://doi.org/10.1111/j.1502-3885.2001.tb01223.x, 2001.
- Bevan, S. L., Luckman, A. J., and Murray, T.: Glacier dynamics over the last quarter of a century at Helheim, Kangerdlugssuaq and 14 other major Greenland outlet glaciers, The Cryosphere, 6, 923–937, https://doi.org/10.5194/tc-6-923-2012, 2012.
- Böcher, J., and Bennike, O.: Early Holocene insect and plant remains from Jameson Land, East Greenland, Boreas, 25, 187–193, https://doi.org/10.1111/j.1502-3885.1996.tb00847.x, 1996.
- Briner, J. P., Cuzzone, J. K., Badgeley, J. A., Young, N. E., Steig, E. J., Morlighem, M., Schlegel, N. J., Hakim, G. J., Schaefer, J. M., Johnson, J. V., Lesnek, A. J., Thomas, E. K., Allan, E., Bennike, O., Cluett, A. A., Csatho, B., de Vernal, A., Downs, J., Larour, E., and Nowicki, S.: Rate of mass loss from the Greenland Ice Sheet will exceed Holocene values this century, Nature, 586, 70–74, https://doi.org/10.1038/s41586-020-2742-6, 2020.
- Cage, A. G., Pieńkowski, A. J., Jennings, A., Knudsen, K. L., and Seidenkrantz, M.-S.: Comparative analysis of six common foraminiferal species of the genera Cassidulina, Paracassidulina, and Islandiella from the Arctic–North Atlantic domain, J. Micropalaeontol., 40, 37–60, https://doi.org/10.5194/jm-40-37-2021, 2021.
- Clark, P. U., Dyke, A. S., Shakun, J. D., Carlson, A. E., Clark, J., Wohlfarth, B., Mitrovica, J. X., Hostetler, S. W., and Mc-Cabe, A. M.: The Last Glacial Maximum, Science, 325, 710–714, https://doi.org/10.1126/science.1172873, 2009.
- Consolaro, C., Rasmussen, T. L., and Panieri, G.: Palaeoceanographic and environmental changes in the eastern Fram Strait during the last 14,000 years based on benthic and planktonic foraminifera, Mar. Micropaleontol., 139, 84–101, 2018.
- Cremer, H., Wagner, B., Melles, M., and Hubberten, H. W.: The postglacial environmental development of Raffles Sø, East Greenland: inferences from a 10,000 year diatom record, Journal of Paleolimnology, 26, 67–87, https://doi.org/10.1023/A:1011179321529, 2001.
- Cuzzone, J. K., Young, N. E., Morlighem, M., Briner, J. P., and Schlegel, N.-J.: Simulating the Holocene deglaciation across a marine-terminating portion of southwestern Greenland in response to marine and atmospheric forcings, The Cryosphere, 16, 2355–2372, https://doi.org/10.5194/tc-16-2355-2022, 2022.
- Davies, J., Mathiasen, A. M., Kristiansen, K., Hansen, K. E., Wacker, L., Alstrup, A. K. O., Munk, O. L., Pearce, C., and Seidenkrantz, M. S.: Linkages between ocean circulation and the Northeast Greenland Ice Stream in the Early Holocene, Quaternary Science Reviews, 286, https://doi.org/10.1016/j.quascirev.2022.107530, 2022.
- Deschamps, P., Durand, N., Bard, E., Hamelin, B., Camoin, G., Thomas, A. L., Henderson, G. M., Okuno, J., and Yokoyama, Y.: Ice-sheet collapse and sea-level rise at the Bølling warming 14,600 years ago, Nature, 483, 559–564.,https://doi.org/10.1038/nature10902, 2012.
- Dowdeswell, J. A., Uenzelmann-Neben, G., Whittington, R. J., and Marienfeld, P.: The Late Quaternary sedimentary record in Scoresby Sund, East Greenland, Boreas, 23, 294–310, https://doi.org/10.1111/j.1502-3885.1994.tb00602.x, 1994.

- Dyke, L. M., Hughes, A. L. C., Murray, T., Hiemstra, J. F., Andresen, C. S., and Rodés, Á.: Evidence for the asynchronous retreat of large outlet glaciers in southeast Greenland at the end of the last glaciation, Quaternary Science Reviews, 99, 244-259, https://doi.org/10.1016/j.quascirev.2014.06.001, 2014.
- Evans, J., Cofaigh, C. O., Dowdeswell, J. A., and Wadhams, P.: Marine geophysical evidence for former expansion and flow of the Greenland Ice Sheet across the north-east Greenland continental shelf, Journal of Quaternary Science, 24, 279-293, https://doi.org/10.1002/jqs.1231, 2009.
- Evans, J., Dowdeswell, J. A., Grobe, H., Niessen, F., Stein, R., Hubberten, H.-W., and Whittington, R. J.: Late quaternary sedimentation in Kejser Franz Joseph Fjord and the continental margin of east Greenland, Geol. Soc. Spec. Publ., 203, 149e179. https://doi.org/10.1144/GSL.SP.2002.203.01.09, 2002.
- Funder, S.: Holocene stratigraphy and vegetation history in the Scoresby Sund area, East Greenland, Bulletin Grønlands Geologiske Undersøgelse, 129, 1-66, https://doi.org/10.34194/bullggu.v129.6671, 1978.
- Funder, S. and Hansen, L.: The Greenland ice sheet a model for its culmination and decay during and after the last glacial maximum, Bulletin of the Geological Society of Denmark, 42, 137-152, https://doi.org/10.37570/bgsd-1995-42-12, 1996.
- Funder, S., Kjeldsen, K. K., Kjær, K. H., and O Cofaigh, C.: The Greenland Ice Sheet During the Past 300,000 Years: A Review, Developments in Quaternary Science, 15, https://doi.org/10.1016/B978-0-444-53447-7.00050-7, 2011.
- Funder, S. V.: Scoresby Sund, sheet 12, Descriptive text to Quaternary map of Greenland https://researchprofiles.ku.dk/en/publications/ 500.000, scoresby-sund-sheet-12-descriptive-text-to-quaternary-map-of-gree/ Ingólfsson, Ó., Lyså, A., Funder, S., Möller, P., and Björck, (last access: 3 November 2025), 1990.
- Gulliksen, S., Heinemeier, J., Nydal, R., Rud, N., Skog, G., Thomsen, M. S., and Funder, S.: 14C dating of samples collected during PONAM expeditions to east Greenland. The Last Interglacial-Glacial Cycle: Preliminary Report of the PONAM Fieldwork in Jameson Land and Scorseby Sund, East Greenland, Lundqua Report, 33, 177–181, 1991.
- Håkansson, S.: University of Lund radiocarbon dates IX, Radiocarbon, 18, 290-320, https://doi.org/10.1017/S0033822200003179, 1976.
- Håkansson, L., Briner, J., Alexanderson, H., Aldahan, A., and Possnert, G.: <sup>10</sup>Be ages from central east Greenland constrain the extent of the Greenland ice sheet during the Last Glacial Maximum, Quaternary Science Reviews, 26, 2316–2321, https://doi.org/10.1016/j.quascirev.2007.08.001, 2007a.
- Håkansson, L., Graf, A., Strasky, S., Ivy-ochs, S., Kubik, P. W., Hjort, C., and Schlüchter, C.: Cosmogenic <sup>10</sup>Beages from the Store Koldewey island, NE Green land, Geografiska Annaler Series A. Physical Geography, 89, 195-202, https://doi.org/10.1111/j.1468-0459.2007.00318.x, 2007b.
- Hall, B., Baroni, C., Denton, G., Kelly, M. A., and Lowell, T.: Relative sea-level change, Kjove Land, Scoresby Sund, East Greenland: Implications for seasonality in Younger Dryas time, Quaternary Science Reviews, 27, 2283-2291, https://doi.org/10.1016/j.quascirev.2008.08.001, 2008.
- Hall, B. L., Baroni, C., and Denton, G. H.: Relative sealevel changes, Schuchert Dal, East Greenland, with implications for ice extent in late-glacial and Holocene

- times, Quaternary Science Reviews, 29, 3370–3378, https://doi.org/10.1016/j.quascirev.2010.03.013, 2010.
- Hanebuth, T., Stattegger, K., and Grootes, P. M.: Rapid Flooding of the Sunda Shelf: A Late-Glacial Sea-Level Record, Science, 12, https://doi.org/10.1126/science.288.5468.1033, 2000.
- Hansen, K. E., Lorenzen, J., Davies, J., Wacker, L., Pearce, C., and Seidenkrantz, M. S.: Deglacial to Mid Holocene environmental conditions on the northeastern Greenland shelf, western Fram Strait, Quaternary Science Reviews, 293, https://doi.org/10.1016/j.quascirev.2022.107704, 2022.
- Hansen, L.: Landscape and coast development of a lowland fjord margin following deglaciation, east greenland, Geografiska Annaler: Series A, Physical Geography, 83, 131–144, https://doi.org/10.1111/j.0435-3676.2001.00149.x, 2001.
- Heaton, T. J., Köhler, P., Butzin, M., Bard, E., Reimer, R. W., Austin, W. E. N., Bronk Ramsey, C., Grootes, P. M., Hughen, K. A., Kromer, B., Reimer, P. J., Adkins, J., Burke, A., Cook, M. S., Olsen, J., and Skinner, L. C.: Marine20 - The Marine Radiocarbon Age Calibration Curve (0-55,000 cal BP), Radiocarbon, 62, 779-820, https://doi.org/10.1017/RDC.2020.68, 2020.
- Hughes, A. L. C., Rainsley, E., Murray, T., Fogwill, C. J., Schnabel, C., and Xu, S.: Rapid response of Helheim Glacier, southeast Greenland, to early Holocene climate warming, Geology, 40, 427-430, https://doi.org/10.1130/G32730.1, 2012.
- Hvidberg, C. S., Grinsted, A., Dahl-Jensen, D., Khan, S. A., Kusk, A., Andersen, J. K., Neckel, N., Solgaard, A., Karlsson, N. B., Kjær, H. A., and Vallelonga, P.: Surface velocity of the Northeast Greenland Ice Stream (NEGIS): assessment of interior velocities derived from satellite data by GPS, The Cryosphere, 14, 3487-3502, https://doi.org/10.5194/tc-14-3487-2020, 2020.
- S.: Late Quaternary glacial history of the central west coast of Jameson Land, East Greenland, Boreas, 23, 447-458, https://doi.org/10.1111/j.1502-3885.1994.tb00612.x, 1994.
- IPCC: Climate Change 2021: The Physical Science Basis. Contribution of Working Group 1 to the Sixth Assessment Report of the Intergovernmental Panel on Climate Change, Cambridge University Press, https://doi.org/10.1017/9781009157896, 2021.
- Ivy-Ochs, S. and Briner, J. P.: Dating Disappearing Ice with Cosmogenic Nuclides, Elements, 10, 351-356, https://doi.org/10.2113/gselements.10.5.351, 2014.
- Jakobsson, M., Mohammad, R., Karlsson, M., et al.: The International Bathymetric Chart of the Arctic Ocean Version 5.0, Scientific Data, 11, 1420, https://doi.org/10.1038/s41597-024-04278w. 2024.
- Jennings, A. E., Hald, M., Smith, M., and Andrews, J. T. Freshwater forcing from the Greenland Ice Sheet during the Younger Dryas: Evidence from southeastern Greenland shelf cores, Quaternary Science Reviews, 25, 282-298, https://doi.org/10.1016/j.quascirev.2005.04.006, 2006.
- Jennings, A. E., Knudsen, K. L., Hald, M., Hansen, C. V., and Andrews, J. T.: A mid-Holocene shift in Arctic sea-ice variability on the East Greenland Shelf, The Holocene, 12, 49-58, https://doi.org/10.1191/0959683602hl519rp, 2002.
- Joughin, I., Smith, B. E., Shean, D. E., and Floricioiu, D.: Brief Communication: Further summer speedup of Jakobshavn Isbræ, The Cryosphere, 8, 209-214, https://doi.org/10.5194/tc-8-209-2014, 2014.

- Kelly, M. and Bennike, O.: Quaternary geology of western and central North Greenland, Rapport Grønlands Geologiske Undersøgelse, 153, 1–34, https://doi.org/10.34194/rapggu.v153.8164, 1992
- Kelly, M. A., Lowell, T. V., Hall, B. L., Levy, L. B., Smith, C. A., Salamido, K., Schwartz, R., and Howley, J. A.: Relative summer temperature changes from glacial fluctuations in the Scoresby Sund region, Central East Greenland, during late-glacial time, Quaternary Science Reviews, 367, 109531, https://doi.org/10.1016/j.quascirev.2025.109531, 2025.
- Kelly, M. A., Lowell, T. V., Hall, B. L., Schaefer, J. M., Finkel, R. C., Goehring, B. M., Alley, R. B., and Denton, G. H.: A <sup>10</sup>Be chronology of lateglacial and Holocene mountain glaciation in the Scoresby Sund region, east Greenland: implications for seasonality during lateglacial time, Quaternary Science Reviews, 27, 2273–2282, https://doi.org/10.1016/j.quascirev.2008.08.004, 2008.
- Khan, S. A., Colgan, W., Neumann, T. A., van den Broeke, M. R., Brunt, K. M., Noël, B., Bamber, J. L., Hassan, J., and Bjørk, A. A.: Accelerating Ice Loss From Peripheral Glaciers in North Greenland, Geophysical Research Letters, 49, https://doi.org/10.1029/2022GL098915, 2022.
- Kokfelt, T. F., Willerslev, E., Bjerager, M., Heijboer, T., Keulen, N., Larsen, L. M., Pedersen, C. B., Pedersen, M., Weng, W. L., Walentin, K. T., Sønderholm, M., and Svennevig, K.: Digital 1:500000 scale geological map of Greenland, version 2.0, https://doi.org/10.22008/FK2/FWX5ET, 2023.
- Lal, D.: Cosmic ray labeling of erosion surfaces: in situ nuclide production rates and erosion models, Earth and Planetary Science Letters, 104, 424–439, 1991.
- Landvik, J. Y.: The last glaciation of Germania Land and adjacent areas, northeast Greenland, Journal of Quaternary Science, 9, 81–92, https://doi.org/10.1002/jqs.3390090108, 1994.
- Larsen, N. K., Funder, S., Kjær, K. H., Kjeldsen, K. K., Knudsen, M. F., and Linge, H.: Rapid early Holocene ice retreat in West Greenland, Quaternary Science Reviews, 92, 310–323, https://doi.org/10.1016/j.quascirev.2013.05.027, 2014.
- Larsen, N. K., Levy, L. B., Carlson, A. E., Buizert, C., Olsen, J., Strunk, A., Bjørk, A. A., and Skov, D. S.: Instability of the Northeast Greenland Ice Stream over the last 45,000 years, Nature Communications, 9, https://doi.org/10.1038/s41467-018-04312-7, 2018.
- Larsen, N. K., Søndergaard, A. S., Levy, L. B., Olsen, J., Strunk, A., Bjørk, A. A., and Skov, D.: Contrasting modes of deglaciation between fjords and inter-fjord areas in eastern North Greenland, Boreas, 49, 903–917, https://doi.org/10.1111/bor.12475, 2020.
- Larsen, N. K., Søndergaard, A. S., Levy, L. B., Strunk, A., Skov, D. S., Bjørk, A., Khan, S. A., and Olsen, J.: Late glacial and Holocene glaciation history of North and Northeast Greenland, Arctic, Antarctic, and Alpine Research, 54, 294–313, https://doi.org/10.1080/15230430.2022.2094607, 2022.
- Leger, T. P. M., Clark, C. D., Huynh, C., Jones, S., Ely, J. C., Bradley, S. L., Diemont, C., and Hughes, A. L. C.: A Greenlandwide empirical reconstruction of paleo ice sheet retreat informed by ice extent markers: PaleoGrIS version 1.0, Clim. Past, 20, 701–755, https://doi.org/10.5194/cp-20-701-2024, 2024.
- Lesnek, A. J., Briner, J. P., Young, N. E., and Cuzzone, J. K.: Maximum Southwest Greenland Ice Sheet Recession

- in the Early Holocene, Geophysical Research Letters, 47, https://doi.org/10.1029/2019GL083164, 2020.
- Levy, L. B., Kelly, M. A., Howley, J. A., and Virginia, R. A.: Age of the Ørkendalen moraines, Kangerlussuaq, Greenland: Constraints on the extent of the southwestern margin of the Greenland Ice Sheet during the Holocene, Quaternary Science Reviews, 52, 1–5, https://doi.org/10.1016/j.quascirev.2012.07.021, 2012.
- Levy, L. B., Kelly, M. A., Lowell, T. V., Hall, B. L., Howley, J. A., and Smith, C. A.: Coeval fluctuations of the Greenland ice sheet and a local glacier, central East Greenland, during late glacial and early Holocene time, Geophysical Research Letters, 43, 1623–1631, https://doi.org/10.1002/2015GL067108, 2016.
- Long, A. J., Roberts, D. H., and Dawson, S.: Early Holocene history of the west Greenland Ice Sheet and the GH-8.2 event, Quaternary Science Reviews, 25, 904–922, https://doi.org/10.1016/j.quascirev.2005.07.002, 2006.
- López-Quirós, A., Junna, T., Davies, J., Andresen, K. J., Nielsen, T., Haghipour, N., Wacker, L., Olsen Alstrup, A. K., Munk, O. L., Rasmussen, T. L., Pearce, C., and Seidenkrantz, M. S.: Retreat patterns and dynamics of the former Norske Trough ice stream (NE Greenland): An integrated geomorphological and sedimentological approach, Quaternary Science Reviews, 325, https://doi.org/10.1016/j.quascirev.2023.108477, 2024.
- Marienfeld, P.: Evolution of sedimentation in Scoresby Sund, East-Greenland during the Holocene, PhD thesis, University of Bremen, https://doi.org/10013/epic.10096.d001, 1991.
- Mienert, J., Andrews, J. T., and Milliman, J. D.: The East Greenland continental margin (65 N) since the last deglaciation: Changes in seafloor properties and ocean circulation, Marine Geology, 106, 217–238, https://doi.org/10.1016/0025-3227(92)90131-Z, 1992.
- Mouginot, J., Rignot, E., Scheuchl, B., Fenty, I., Khazendar, A., Morlighem, M., Buzzi, A., and Paden, J.: Fast retreat of Zachariæ Isstrøm, northeast Greenland, Science, 350, 1357–1361, https://doi.org/10.1126/science.aac7111, 2015.
- Mouginot, J., Bjørk, A. A., Millan, R., Scheuchl, B., and Rignot, E.: Insights on the Surge Behavior of Storstrømmen and L. Bistrup Bræ, Northeast Greenland, Over the Last Century, Geophysical Research Letters, 45, 11197–11205, https://doi.org/10.1029/2018GL079052, 2018.
- NGRIP members: High-resolution record of Northern Hemisphere climate extending into the last interglacial period, Nature, 431, 147–151, https://doi.org/10.1038/nature02805, 2004.
- Nishiizumi, K., Winterer, E. L., Kohl, C. P., Klein, J., Middleton, R., Lal, D., and Arnold, J. R.: Cosmic ray production rates of <sup>10</sup>Be and 26Al in quartz from glacially polished rocks, Journal of Geophysical Research: Solid Earth, 94, 17907–17915, 1989.
- Nishiizumi, K., Imamura, M., Caffee, M. W., Southon, J. R., Finkel, R. C., and McAninch, J.: Absolute calibration of <sup>10</sup>Be AMS standards, Nuclear Instruments and Methods in Physics Research Section B: Beam Interactions with Materials and Atoms, 258, 403–413, https://doi.org/10.1016/j.nimb.2007.01.297, 2007.
- Ó Cofaigh, C., Dowdeswell, J. A., Evans, J., Kenyon, N. H., Taylor, J., Mienert, J., and Wilken, M.: Timing and significance of glacially influenced mass-wasting in the submarine channels of the Greenland Basin, Marine Geology, 207, 39–54, https://doi.org/10.1016/j.margeo.2004.02.009, 2004.
- Ó Cofaigh, C., Lloyd, J. M., Callard, S. L., Gebhardt, C., Streuff, K. T., Dorschel, B., Smith, J. A., Lane, T. P., Jamieson, S. S. R.,

- Kanzow, T., and Roberts, D. H.: Shelf-edge glaciation offshore of northeast Greenland during the last glacial maximum and timing of initial ice-sheet retreat, Quaternary Science Reviews, 359, 109326, https://doi.org/10.1016/j.quascirev.2025.109326, 2025.
- Olsen, I. L., Rydningen, T. A., Forwick, M., Laberg, J. S., and Husum, K.: Last glacial ice sheet dynamics offshore NE Greenland a case study from Store Koldewey Trough, The Cryosphere, 14, 4475–4494, https://doi.org/10.5194/tc-14-4475-2020, 2020.
- Olsen, I. L., Laberg, J. S., Forwick, M., Rydningen, T. A., and Husum, K.: Late Weichselian and Holocene behavior of the Greenland Ice Sheet in the Kejser Franz Josef Fjord system, NE Greenland, Quaternary Science Reviews, 284, https://doi.org/10.1016/j.quascirev.2022.107504, 2022.
- O'Regan, M., Cronin, T. M., Reilly, B., Alstrup, A. K. O., Gemery, L., Golub, A., Mayer, L. A., Morlighem, M., Moros, M., Munk, O. L., Nilsson, J., Pearce, C., Detlef, H., Stranne, C., Vermassen, F., West, G., and Jakobsson, M.: The Holocene dynamics of Ryder Glacier and ice tongue in north Greenland, The Cryosphere, 15, 4073–4097, https://doi.org/10.5194/tc-15-4073-2021, 2021.
- Pearce, C., Özdemir, K. S., Forchhammer Mathiasen, R., Detlef, H., and Olsen, J.: The marine reservoir age of Greenland coastal waters, Geochronology, 5, 451–465, https://doi.org/10.5194/gchron-5-451-2023, 2023.
- Rasmussen, S. O., Andersen, K. K., Svensson, A. M., Steffensen,
  J. P., Vinther, B. M., Clausen, H. B., Siggaard-Andersen, M.
  L., Johnsen, S. J., Larsen, L. B., Dahl-Jensen, D., Bigler, M.,
  Röthlisberger, R., Fischer, H., Goto-Azuma, K., Hansson, M.
  E., and Ruth, U.: A new Greenland ice core chronology for the
  last glacial termination, Journal of Geophysical Research Atmospheres, 111, https://doi.org/10.1029/2005JD006079, 2006.
- Reeh, N., Bøggild, C. E., and Oerter, H.: Surge of Storstrømmen, a large outlet glacier from the Inland lee of North-Bast Greenland, Rapport Grønlands Geologiske Undersøgelse, 162, 201–209, https://doi.org/10.34194/rapggu.v162.8263, 1994.
- Reimer, P. J. and Reimer, R. W.: A marine reservoir correction database and on-line interface, Radiocarbon, 43, 461–463, https://doi.org/10.1017/s0033822200038339, 2001.
- Reimer, P. J., Austin, W., Bard, E., Bayliss, A., Blackwell, P. G., Ramsey, C. B., Butzin, M., Cheng, H., Edwards, R. L., Friedrich, M., Grootes, P. M., Guilderson, T. P., Hajdas, I., Heaton, T. J., Hogg, A. G., Hughen, K. A., Kromer, B., Manning, S. W., Muscheler, R., Palmer, J. G., Pearson, C., van der Plicht, J., Reimer, R. W., Richards, D. A., Scott, E. M., Southon, J. R., Turney, C. S. M., Wacker, L., Adolphi, F., Büntgen, U., Capano, M., Fahrni, S., Fogtmann-Schulz, A., Friedrich, R., Köhler, P., Kudsk, S., Miyake, F., Olsen, J., Reinig, F., Sakamoto, M., Sookdeo, A., and Talamo, S.: The IntCal20 Northern Hemisphere Radiocarbon Age Calibration Curve (0–55 cal kBP), Radiocarbon, 62, 725–757, https://doi.org/10.1017/RDC.2020.41, 2020.
- Rignot, E., Bjork, A., Chauche, N., and Klaucke, I.: Storstrømmen and L. Bistrup Bræ, North Greenland, Protected From Warm Atlantic Ocean Waters, Geophysical Research Letters, 49, https://doi.org/10.1029/2021GL097320, 2022.
- Roberts, D. H., Lane, T. P., Jones, R. S., Bentley, M. J.,
  Darvill, C. M., Rodes, A., Smith, J. A., Jamieson, S. S.
  R., Rea, B. R., Fabel, D., Gheorghiu, D., Davidson, A.,
  Cofaigh, C., Lloyd, J. M., Callard, S. L., and Humbert,
  A.: The deglacial history of 79N glacier and the North-

- east Greenland Ice Stream, Quaternary Science Reviews, 336, https://doi.org/10.1016/j.quascirev.2024.108770, 2024.
- Schaefer, J. M., Denton, G. H., Kaplan, M., Putnam, A., Finkel, R. C., Barrell, D. J. A., Andersen, B. G., Schwartz, R., Mackintosh, A., Chinn, T., and Schlüchter, C.: High-Frequency Holocene Glacier Fluctuations in New Zealand Differ from the Northern Signature, Science, 324, 622–625, https://doi.org/10.1126/science.1169312, 2009.
- Skov, D. S., Andersen, J. L., Olsen, J., Jacobsen, B. H., Knudsen, M. F., Jansen, J. D., Larsen, N. K., and Egholm, D. L.: Constraints from cosmogenic nuclides on the glaciation and erosion history of Dove Bugt, northeast Greenland, Bulletin of the Geological Society of America, 132, 2282–2294, https://doi.org/10.1130/b35410.1, 2020.
- Smith, L. M. and Anderson, J. B.: Radiocarbon Date List IX, Antarctica, Arctic Ocean, and the Northern North Atlantic Region (No. 54), Institute of Arctic and Alpine Research, University of Colorado, Boulder, Colorado, 146 pp., 2000.
- Stein, R., Nam, S. I., Grobe H., and Hubberton, H.: Late Quaternary glacial history and short-term ice-rafted debris fluctuations along the East Greenland continental margin, Geological Society, London, Special Publication, 111, 135–151, https://doi.org/10.1144/GSL.SP.1996.111.01.09, 1996.
- Stone, J. O.: Air pressure and cosmogenic isotope production, Journal of Geophysical Research: Solid Earth, 105, 23723–23753, 2000.
- Stuiver, M. and Reimer, P. J.: Extended <sup>14</sup>C data base and revised CALIB 3.0 <sup>14</sup>C age calibration program, Radiocarbon, 35, 215–230, https://doi.org/10.1017/S0033822200013904, 1993.
- Syring, N., Lloyd, J. M., Stein, R., Fahl, K., Roberts, D. H., Callard, L., and O'Cofaigh, C.: Holocene interactions between glacier retreat, sea ice formation, and Atlantic water advection at the inner Northeast Greenland continental shelf, Paleoceanography and Paleoclimatology, 35, e2020PA004019, https://doi.org/10.1029/2020PA004019, 2020.
- The IMBIE Team: Mass balance of the Greenland Ice Sheet from 1992 to 2018, Nature, 579, 233–239, https://doi.org/10.1038/s41586-019-1855-2, 2020.
- Vijay, S., Khan, S. A., Kusk, A., Solgaard, A. M., Moon, T., and Bjørk, A. A.: Resolving Seasonal Ice Velocity of 45 Greenlandic Glaciers With Very High Temporal Details, Geophysical Research Letters, 46, 1485–1495, https://doi.org/10.1029/2018GL081503, 2019.
- Wager, L. R.: Geological investigations in East Greenland. Part IV: The Stratigraphy and Tectonics of Knud Rasmussens Land and the Kangerdlugssuqq Region, Meddelelser Om Grønland, 134, 1–64, 1947.
- Wagner, B. and Melles, M.: Holocene environmental history of western Ymer Ø, East Greenland, inferred from lake sediments, Quatern. Int., 89, 165–176, https://doi.org/10.1016/S10406182(01)00087-8, 2002.
- Weidick, A.: C14 dating of Survey material carried out in 1976, Rapp. Grønlands Geol. Undersøgelse, 85, 127–129, https://doi.org/10.34194/rapggu.v85.7545, 1977.
- Weidick, A.: C14 dating of survey material carried out in 1977, Rapp. Grønlands Geol. Undersøgelse, 90, 119–124, https://doi.org/10.34194/rapggu.v90.7609, 1978.
- Weidick, A., Andreasen, C., Oerter, H., and Reeh, N.: Neoglacial Glacier Changes around Storstremmen, North-East Greenland,

- Polarforschung, 64, 95–108, https://doi.org/10013/epic.13889, 1996.
- Williams, K. M.: Ice sheet and ocean interactions, margin of the East Greenland Ice Sheet (14 ka to present): Diatom evidence, Paleoceanography, 8, 69–83, https://doi.org/10.1029/92PA02591,1993.
- Williams, K. M., Andrews, J. T., Weiner, N. J. and Mudie, P. J.: Late Quaternary paleoceanography of the mid-to outer continental shelf, East Greenland, Arctic and Alpine Research, 27, 352– 363, https://doi.org/10.1080/00040851.1995.12003132, 1995.
- Wilson, N., Straneo, F., and Heimbach, P.: Satellite-derived submarine melt rates and mass balance (2011–2015) for Greenland's largest remaining ice tongues, The Cryosphere, 11, 2773–2782, https://doi.org/10.5194/tc-11-2773-2017, 2017.
- Young, N. E., Briner, J. P., Stewart, H. A. M., Axford, Y., Csatho, B., Rood, D. H., and Finkel, R. C.: Response of Jakobshavn Isbræ, Greenland, to Holocene climate change, Geology, 39, 131–134, https://doi.org/10.1130/G31399.1, 2011.
- Young, N. E., Briner, J. P., Rood, D. H., Finkel, R. C., Corbett, L. B., and Bierman, P. R.: Age of the Fjord Stade moraines in the Disko Bugt region, western Greenland, and the 9.3 and 8.2 ka cooling events, Quaternary Science Reviews, 60, 76–90, https://doi.org/10.1016/j.quascirev.2012.09.028, 2013a.

- Young, N. E., Schaefer, J. M., Briner, J. P., and Goehring, B. M.: A <sup>10</sup>Be production-rate calibration for the Arctic, Journal of Quaternary Science, 28, 515–526, https://doi.org/10.1002/jqs.2642, 2013b.
- Young, N. E., Briner, J. P., Miller, G. H., Lesnek, A. J., Crump, S. E., Thomas, E. K., Pendleton, S. L., Cuzzone, J., Lamp, J., Zimmerman, S., Caffee, M., and Schaefer, J. M.: Deglaciation of the Greenland and Laurentide ice sheets interrupted by glacier advance during abrupt coolings, Quaternary Science Reviews, 229, https://doi.org/10.1016/j.quascirev.2019.106091, 2020.
- Young, N. E., Briner, J. P., Miller, G. H., Lesnek, A. J., Crump, S. E., Pendleton, S. L., Schwartz, R., and Schaefer, J. M.: Pulsebeat of early Holocene glaciation in Baffin Bay from high-resolution beryllium-10 moraine chronologies, Quaternary Science Reviews, 270, https://doi.org/10.1016/j.quascirev.2021.107179, 2021.